An explanation of the relationships between mass, metabolic rate and characteristic length for placental mammals

Charles C. Frasier

Organizationally unaffiliated in San Diego, California, United States of America

Abstract. The Mass, Metabolism and Length Explanation (MMLE) was advanced in 1984 to explain the relationship between metabolic rate and body mass for birds and mammals. This paper reports on a modernized version of MMLE. MMLE predicts the absolute value of Basal Metabolic Rate (BMR) for individual animals rather than parameters in the power law relationship BMR = a(body mass)^{b}. Beginning with the proposition that BMR is proportional to the number of mitochondria in an animal, two primary equations are derived that predict BMR and body mass as functions of an individual animal's characteristic length and sturdiness factor. The characteristic length is a measureable skeletal length associated with an animal's means of propulsion. The sturdiness factor expresses how sturdy or gracile an animal is. Eight other parameters occur in the equations that vary little among animals in the same phylogenetic group. The present paper modernizes MMLE by explicitly treating Froude and Strouhal dynamic similarity of mammals' skeletal musculature, revising the treatment of BMR and using new data to estimate numerical values for the parameters that occur in the equations. A mass and length data set with 575 entries from the orders Rodentia, Chiroptera, Artiodactyla, Carnivora, Perissodactyla and Proboscidae is used. A BMR and mass data set with 436 entries from the orders Rodentia, Chiroptera, Artiodactyla and Carnivora is also used. With the estimated parameter values MMLE can exactly predict every BMR and mass datum from the BMR and mass data set without any unexplained variance. Furthermore MMLE can exactly predict every body mass and length datum from the mass and length data set without any unexplained variance. Whether or not MMLE can simultaneously exactly predict an individual animal's BMR and body mass given its characteristic length awaits analysis of a data set that simultaneously reports all three of these items for individual animals.

PeerJ PrePrints | http://dx.doi.org/10.7287/peerj.preprints.437v1 | CC-BY 4.0 Open Access | received: 12 Jul 2014, published: 12 Jul

Introduction. Most theoretical treatments of Basal Metabolic Rate (BMR) have focused on the exponent in a relationship of the form BMR = aW^b where W is body mass. Two concepts have dominated. One concept is geometric similarity in which the value of the exponent b = 2/3. The theoretical explanations for this value of the exponent generally involve a balance between heat production and its loss through the body surface (Hulbert & Else, 2004; Clarke, Rothery & Isaac, 2010; Roberts, Lightfoot & Porter, 2010; White, 2010; Roberts, Lightfoot & Porter, 2011; Seymour & White, 2011). In the other concept b = 3/4 (Kleiber, 1932; Kleiber, 1961). This has been known as "Kleiber's Law". A theoretical explanation for b = 3/4 was proposed based on a fractal network for a body's resource supply system (Seymour & White, 2011). More recently theoretical explanations involving resource distribution networks for which the value of the exponent b can be as small as 2/3 or as large as 3/4 have been proposed (Banavar et al. 2010). The metabolic-level boundaries hypothesis proposes that the exponent b is proportional to the proportions of influence of volume and surface area boundary constraints and thus has a value between 2/3 and 1.0 (Glazier, 2010).

More microscopically, it has been proposed that an animal's BMR is proportional to the total number of mitochondria in its tissues (Smith, 1956) or to the sum of the metabolic rates of its constituent cells (Kozlowski, Konarzewski & Gawelczyk, 2003). At an even smaller scale it has been proposed in membrane pacemaker theory (Hulbert & Else, 1999) that BMR is governed by the degree of polyunsaturation of membrane phospholipids or, in the Quantum Metabolism theory (Agutter & Tuszynski, 2011), by molecular-cellular processes.

Recent analyses of BMR, body mass data have argued that there is no single exponent b that applies to a phylogenetic class such as mammals. The relationship is more complicated than BMR = aW^b (Kolokotrones et al, 2010). It has also been argued that there are different exponents for different phylogenetic groups such as mammal orders (White, Blackburn & Seymour, 2009; Capellini, Venditti & Barton, 2010)or different orders among insects, fish, reptiles and birds as well as mammals (Isaac & Carbone, 2010).

The dynamic energy budget (DEB) hypothesis (Sousa et al, 2010; White CR et al, 2011; Maino et al, 2014) can predict the absolute value of BMR rather than the exponent b in the relationship aW^b.

In 1984 the author of the current paper proposed the Mass, Metabolism and Length Explanation (MMLE) theory that also predicts the absolute value of BMR rather than just the exponent b in the relationship BMR = aW^b (Frasier, 1984). A purpose of developing MMLE theory was to relate BMR to measurable skeletal dimensions with the hope of estimating the BMR of extinct animals. Starting with the (Smith, 1956) proposal that an animal's BMR is proportional to the total number of mitochondria in its tissues the theoretical derivation took a course that resulted in equations for predicting the absolute value of body mass as a function of a skeletal length dimension as well as predicting the absolute value of BMR as a function of that skeletal

dimension. Used together these equations can predict the absolute value of BMR as a function of body mass. This paper will frequently be referred to as the 'original paper' in the present paper.

McNab (McNab, 1988) questioned what should be the best measure of body size against which to scale various functions such as BMR. He presented good reasons why body mass is more variable than linear dimensions in adult mammals. Nevertheless McNab concluded that he would use body mass for want of a better measure of body size. Mass may be an even less reliable measure of body size among bats in which it may vary by as much as 15% to 50% daily (Iriarte-Diaz et al, 2012).

The simplest relationship between body mass and a skeletal length dimension would be geometric similarity in which body mass would be proportional to the cube of the length or, equivalently, the length would be proportional to the cube root of the mass. However Galileo, as cited in (Christiansen, 1999; Biewener, 2005), recognized in 1638 that geometric similarity implied that small animals would have to be mechanically overbuilt or large animals would have to operate near the limit of mechanical failure. Elastic similarity was proposed as a theoretical solution to this problem (McMahon, 1973; McMahon, 1975) but its predictions did not agree with data (Alexander et al, 1979; Christiansen, 1999). More recently an explanation based on the need of long bones to resist bending and compressive stress has been proposed (Garcia & da Silva, 2004).

It has been recognized that in a relationship relating a skeletal length, l, to body mass raised to an exponent, W^x, the exponent may be different for large terrestrial mammals compared to small terrestrial mammals (Christiansen, 1999; Biewener, 2005). (Campione & Evans, 2013) found that the regression between the total circumference of the humerus and femur to body mass exhibits the strongest relationship with the highest coefficient of determination values; and the lowest mean percent prediction error, standard error of the estimate and Akaike Information Criterion values of all bivariate regression models for exant mammals and reptiles.

These theoretical explanations for the relationship between skeletal length dimensions and body mass are based on the stresses the bones and their supporting tissues must accommodate. MMLE theory went in a different direction by examining the rate of energy use in skeletal muscle tissues during activity and the relationship between muscle energy use and energy use by a body's other tissues in the basal metabolic rate state.

Since the original publication of MMLE the amount of BMR, body mass data has vastly expanded as has the resources with which to analyze it. So the purpose of this paper is to use these resources to revisit MMLE theory and test its ability to predict the absolute values of BMR and body mass for individual animals with the new data. MMLE theory will also be modified as necessary.

The running/walking members of the orders Artiodactyla, Carnivora, Perissodactyla and Proboscidea were addressed in the original paper. The present analysis will add Rodentia and

Chiroptera (bats) as well as redo the runners/walkers analysis with new data. Rodentia are a small animal counterbalance to the large runners/walkers and they comprise over 40% of placental mammal species. A comprehensive theory should be able to address flying animals as well as terrestrials and bats comprise another 20% of placental mammal species. Swimming animals should also be addressed but there is too little BMR and body mass data to generate reliable results for the orders Pinnipedia, Cetacea and Sirenia. While not addressing the entirety of the placental mammals, the orders that are addressed do represent over two-thirds of the species.

Summary of MMLE Theory. This section presents an abbreviated version of MMLE theory as originally formulated (Frasier, 1984) together with some necessary modifications.

Nearly all of the energy flux that is measured as basal metabolic rate (BMR) is generated by mitochondria. Although there are other ways to measure it, BMR is most commonly measured by oxygen consumption (Hulbert & Else, 2004). The oxygen is consumed by processes that pump protons across the mitochondrion inner membrane. Heat is produced when some of the protons leak back across the membrane in a controlled fashion as in brown fat or as an uncontrolled basal leak. Otherwise the protons cause the phosphorylation of adenosine diphosphate (ADP) to adenosine triphosphate (ATP) as they return across the inner membrane (Jastroch et al,.2010). ATP is the fuel that powers animal tissues.

MMLE strives to predict the absolute value of the BMR of an animal rather than the exponent b or the constant a in the relationship aW^b. It calculates BMR by summing the energy allocation to an animal's tissues. The energy allocated to a tissue type is proportional to the number of mitochondria in the tissue. Thus MMLE tries to count the mitochondria in the tissues that compose an animal and then sum these counts for the entire animal. This approach to calculating an animal's BMR was proposed by (Smith, 1956).

MMLE also proposes that mitochondria have a lower limit for the rate of energy release that is experienced by an adult in the thermoneutral zone when inactive and post-absorptive. Basal metabolic rate (BMR) is experienced when an animal's mitochondria are in this state. The lower limit for the rate of energy release by a mitochondrion can be different for different tissue types and different phylogenetic groups.

The skeletal muscles, heart, kidneys, liver and brain dominate BMR for vertebrates. These tissues account for 75% to 81% of BMR in the reference man (Müller et al, 2013). The heart, kidneys, liver and brain account for more than 60% of human BMR while accounting for less than 6% of body mass. The sum of the energy consumption by each of the non-skeletal muscle tissues that dominate BMR appears to scale with body mass with the same exponent b in the relationship $BMR = aW^b$ as does BMR for the entire body even though the energy consumption for each separate tissue type may not (Wang et al, 2001).

Mitochondria are distributed approximately uniformly throughout a muscle. In the other tissues that dominate BMR the mitochondria are distributed in a relatively thin surface that surrounds material containing few mitochondria. The original paper examines the anatomy of the vertebrate liver in detail to show that it is composed of thin surfaces of hepatic cells richly endowed with mitochondria surrounding endothelial linings, blood, bile and other materials with relatively few mitochondria. For these reasons MMLE theory uses a simplified model of a vertebrate's body consisting of two components: 1) volume active tissues in which mitochondria are approximately uniformly distributed throughout the tissue; and 2) surface active tissues in which mitochondria are concentrated in a surface that surrounds materials that contain few mitochondria.

Because the skeletal musculature dominates the volume active tissues from an energy perspective, these tissues were called "skeletal musculature" in the original paper. The surface active tissues that are dominated by the heart, kidneys, liver and brain were called "non-skeletal musculature".

It was argued in the original paper that the density of mitochondria in the cells composing the surface active tissues was the maximum possible consistent with the functioning of the cells. The skeletal musculature is sized to support the mechanical loads imposed by activity. The density of mitochondria in the skeletal musculature is sufficient to support the mechanical power requirements of the activity.

In the BMR state skeletal muscle mitochondria are only supporting local maintenance functions. Mitochondria in the rest of the body may be operating at a greater output level to support their local maintenance functions, the other components of the non-skeletal muscle tissues and the skeletal muscles. Thus the minimum rate of energy release by a mitochondrion should occur with skeletal muscle mitochondria in the BMR state. MMLE uses this possibility to express the rate of energy release by mitochondria in other tissues in the BMR state and in all tissues in non-BMR activity states as amplification constants multiplying the skeletal muscle mitochondrion rate of energy release in the BMR state.

MMLE theory proposed that the minimum rate of energy release by a skeletal muscle mitochondrion in the BMR state can be different for different phylogenetic groups. The original paper assumed that the phylogenetic level at which the difference occurs was the infraclass. The examination of placental mammals later in the current paper indicates that the difference may occur at the level of the family and possibly at the level of the species in some families. Some differences may occur between individuals due to genetic variation within a species.

Mitochondria have different respiration rates in different phylogenetic groups (Else & Hulbert, 1981; Else & Hulbert, 1985; Hulbert & Else, 2004; Guderley et al, 2005). Assuming that the BMR state minimum rate of skeletal mitochondrion energy release is genetically determined, a difference between related phylogenetic groups implies mutations affecting mitochondrion performance. Mutations in mitochondria DNA that could affect ATP production were found in

all of 41 species of mammals that were examined (da Fonseca et al, 2010). But the situation could be more complex as mitochondrial function plastically responds to change through DNA transcription control, mitochondrial membrane composition and proton leak (Seebacher et al, 2010).

Because a value for the minimum rate of energy release by a skeletal muscle mitochondrion in the BMR state was not available, it was replaced by a non-dimensional parameter, e, which was named the 'mitochondrion capability quotient'. The parameter e is defined as the minimum rate of energy release by a skeletal muscle mitochondrion in the BMR state for a particular phylogenetic group relative to the minimum rate of energy release by a skeletal muscle mitochondrion in the BMR state for walking/running placental mammals. This definition will be further restricted when walking/running placental mammals are addressed later in the present paper.

Although it was not addressed in the original paper, the mitochondrion capability quotient should be, among other things, a function of body temperature.

Skeletal muscle mitochondria require the support of the functions powered by the mitochondria in the non-skeletal musculature. MMLE theory considers this to be a constraint in that at levels of muscle activity that can be sustained long term without the accumulation of an oxygen debt, the total power produced by muscle mitochondria is proportional to the total power produced by mitochondria in the non-skeletal musculature. Since the total power produced in a tissue type is (e) X (the number of mitochondria in the tissue) X (the amplification constant appropriate for the tissue and the host animal's activity state), it was concluded the power produced by skeletal muscle mitochondria in the BMR state is also proportional to the power produced by mitochondria in the non-skeletal musculature in the BMR state. Since BMR is the sum of these two power components, BMR is equal to the power produced by mitochondria in the non-skeletal muscle body component multiplied by an appropriate constant.

This summary of MMLE theory will use the term 'appropriate constant' for intermediate constants needed to make an intermediate relationship an equality. When the intermediate relationships have been combined into the final MMLE equations the constants occurring in those equations will be given unique symbols. The mathematically rigorous derivations are available in the original paper.

For skeletal muscle there are additional constraints. The power generated by mitochondria is also proportional to the mechanical power that a muscle must generate during normal activity. The mechanical power is (the force the muscle bears) X (the distance the muscle extends/contracts) X (the frequency of extension/contraction) where each term is evaluated for the host animal's activity state. The power is also proportional to (e) X (the mass specific density of mitochondria in the muscle) X (the muscle's mass) X (the amplification constant appropriate to the activity state of the animal). By analyzing these constraints with respect to the sliding

filament theory of muscle contraction, the MMLE theoretical analysis concluded that they could be simultaneously satisfied if the mass of the skeletal muscles were proportional to BMR divided by the fundamental frequency of muscle activity.

The actual frequency at which a muscle operates is a multiple of the fundamental frequency. The multiplier is a function of an animal's activity state.

Propulsion was considered to be the primary power consuming activity of skeletal muscles for vertebrates. For animals employing similar dynamics for propulsion, muscle mass can be equated to (an appropriate constant) X (BMR) divided by (the fundamental propulsion frequency). To account for different propulsion dynamics, the fundamental frequency was multiplied by yet another appropriate constant.

This was how the original paper recognized that dynamic similarity could be used to scale muscle mass for animals of different sizes. Alexander (Alexander, 2005) addressed dynamic similarity in animals in terms of Froude, Reynolds, and Strouhal similarity. This is a physically more meaningful way to address dynamic similarity. MMLE theory in the present paper is modified to embrace these types of dynamic similarity.

In the non-skeletal muscle tissues that dominate BMR, the mitochondria are distributed in a relatively thin surface that surrounds material containing few mitochondria. Recognizing this, MMLE theory describes the mass of the non-skeletal musculature in terms of the total surface area of the energetically active surfaces.

Being a surface, the non-skeletal muscle surface can be mathematically described as the square of a length multiplied by an appropriate constant. Any length could be used as long as the constant is adjusted to make the relationship exact. For MMLE theory the selected length is one that is related to propulsion dynamics. This selected length is called the 'characteristic length', l. The proportionality constant includes the 'sturdiness factor', s. s is non-dimensional.

It is the expression of the sum of the areas of the metabolically active surfaces of the non-skeletal musculature as proportional to $(sl)^2$ that is the fundamental innovation of MMLE theory.

The foregoing considerations were consolidated to express the mass of the non-skeletal musculature equal to $((sl)^2 mG_o/e)^{1/y}$ where mG_o is the final appropriate proportionality constant. G_o has the same value and physical dimensions for all values of y. m is a dimensionality factor that adjusts the physical dimensions of this expression to mass. m is determined by y. m is not an independent variable. The dimensionality factor, m, was not part of the original paper.

The mass of the skeletal musculature is equal to $(sl)^2 G_m/kfe$ where f is the fundamental frequency of propulsion, and G_m and k are the final appropriate proportionality constants. Since total body mass, W, is the sum of these two components:

$$W = (sl)^2 G_m/kfe + ((sl)^2 mG_o/e)^{1/y} \quad (1)$$

The basal metabolic rate, BMR, is:

$$BMR = G_r(sl)^2 \quad (2)$$

where G_r is the final appropriate proportionality constant.

Surrogate characteristic length and body mass data are available in (Nowak, 1999). It has been entered into Microsoft Excel spread sheets that are available as Supplemental Information Data S1, Data S2 and Data S3. The author of the present paper is unaware of any substantial collection of BMR and characteristic length data. There is substantial BMR and body mass data in (McNab, 2008). These data are also available with additional data as a Microsoft Excel spread sheet in the Supplementary Information for (Kolokotrones et al, 2010) at www.nature.com/nature/journal/v464/n7289/suppinfo/nature08920.html which was the source that was used for the present paper. To use this data, equations (1) and (2) can be used together to numerically express BMR as a function of body mass.

G_o is defined so that m is dimensionless with a value of 1.0 for geometrically similar non-skeletal musculature for which y = 2/3.

The equation for skeletal muscle mass includes two final appropriate constants: G_m and k. k is a function of the type of dynamic similarity that applies to the type of propulsion used by an animal. G_m and k were defined so that k is non-dimensional with a value of 1.0 for running/walking placental mammals.

The dimensions of the final appropriate constants in equations (1) and (2) are physically straight forward. In the meters kilograms seconds (MKS) system of physical units G_m has the dimensions (kg/m^2 sec). G_o has the dimensions ($kg^{2/3}/m^2$) for y = 2/3. m has the dimensions necessary to make the expression for the mass of the non-skeletal musculature in equation (1) have the dimension of mass. G_r has the dimensions ($watts/m^2$). MMLE avoids the physics challenge of the multiplicative constant a in relationships like aW^b when b varies among different phylogenetic groups as was found in (White, Blackburn & Seymour, 2009; Capellini, Venditti & Barton, 2010; Isaac & Carbone, 2010; Hudson, Isaac &, Reuman, 2013).

It is a signature feature of MMLE theory that the vertebrate body is represented as a combination of masses instead of a single mass. There are at least two masses: 1) the skeletal musculature which is governed by dynamic similarity and in which the power producing organelles are approximately uniformly distributed; and 2) the non-skeletal musculature in which the power producing organelles are concentrated in surfaces that surround material with few power producing organelles. This binary nature of the vertebrate body can lead to different exponents in the relationship $BMR = aW^b$ for different phylogenetic groups within the same infraclass. As cited in (Hulbert & Else, 2004) Hemmingsen observed in 1960 that a body composed with this sort of binary distribution of power producing organelles could account for values of the exponent b that are different from the geometric similarity value of 2/3.

In MMLE theory equations (1) and (2) are exact once numerical values for the parameters have been established. G_m, G_o and G_r are universal constants that should apply to all vertebrates. y and m should have the same value for all animals in a phylogenetic group . k is a constant whose value should be similar for all vertebrates that are dynamically similar. The fundamental propulsion frequency, f, should be the same function of the characteristic length, l, for all vertebrates that are dynamically similar. e is a constant whose value should be approximately identical for all vertebrates in the same phylogenetic group with the same body temperature. The characteristic length, l, and the sturdiness factor, s, have unique values for each individual animal.

MMLE thusly uses nine parameters to predict the absolute values of the body mass and BMR of a vertebrate. Nine is the same number of factors that McNab (McNab, 2008) found influenced mammal BMR; and it is less than the over 22 parameters needed to best describe the overall mass and temperature dependence of BMR by the (White, Frappell & Chown, 2012) information-theoretic analysis. While that analysis did include insects, spiders, protists and prokaryotes as well as vertebrates, it and McNab's findings do indicate that needing a large number of parameters to predict the absolute value of a vertebrate's body mass and BMR should not be surprising. Even describing the relationships between BMR and body mass, W, and a skeletal dimension, l, for a collection of animals with the simple relationships $BMR = aW^b$ and $W = dl^x$ requires at least five parameters and as many as six if BMR and length data are not for the same individual animals. Simplicity is not necessarily better than complexity (White, Frappell & Chown, 2012).

In the original paper G_m/k, G_o and G_r were considered nearly invariant among vertebrates so that there were only five degrees of freedom for equations (1) and (2).

In a subsequent section of the current paper numerical values for G_m, G_o and G_r will be determined by analyzing body mass, BMR and characteristic length data for walking/running placental mammals for which k = 1.0 and e = 1.0. To do this the fundamental propulsion frequency, f, needs to be established. After analyzing data for running/walking mammals, rodents and bats a general formulation for the fundamental propulsion frequency appears to be $f = c/l^r$ where c is the appropriate proportionality constant and r is an exponent with a value between 0.5 and 1.0 for species in these mammal orders. Substituting this expression for f in equation (1) yields:

$$W = s^2 l^{(2+r)} G_m/kce + ((sl)^2 mG_o/e)^{1/y} \qquad (3)$$

Animals that are dynamically similar have similar values for the exponent, r.

The formulation of the fundamental frequency as $f = c/l^r$ adds an additional parameters to the number that MMLE uses to predict the absolute values of body mass and BMR for a total of 10 parameters.

With a body mass and characteristic length data set such as (Nowak, 1999), equation (3) is exact because for every datum a value for the sturdiness factor can be found such that the body mass is exactly computed by the equation using this found sturdiness factor and the characteristic length. With a BMR and body mass data set such as (Kolokotrones et al, 2010), equations (2) and (3) are exact because for every datum a value for the sturdiness factor and a value for the characteristic length can be found such that the BMR is exactly computed by equation (2) and the body mass is exactly computed by equation (3) using the found sturdiness factor value and the found characteristic length value.

When the gravitational force dominates the dynamics of animals' movement, two animals are dynamically similar when the ratio of gravitational force to inertial force is the same at corresponding stages of their motions. The animals are Froude similar and they have equal Froude numbers, F, where $F = u^2/gl$ and u is speed, l is the characteristic length and g is the acceleration of gravity which is 9.81 m/sec^2 (Alexander, 2005). Running/walking mammals are Froude similar (Alexander et al, 1979; Alexander, 2005; Raichlen, Pontzer & Shapiro, 2013).

Strouhal similarity obtains when inertial forces are proportional to oscillatory forces. Similarity implies equal Strouhal numbers, St, where $St = fl/u$ and f is the frequency, l is the characteristic length and u is speed. The Strouhal number governs a series of vortex growth and shedding regimes for foils undergoing pitching and heaving motions thereby describing the tail or wing kinematics of swimming or flying animals (Taylor, Nudds & Thomas, 2003).

Reynolds similarity obtains when inertial forces are proportional to viscous forces. Similarity implies equal Reynolds numbers, R, where $R = ul\rho/\nu$ and u is speed, l is characteristic length, ρ is fluid density and ν is fluid viscosity (Alexander, 2005). Bats are the only animals examined in the present paper for which viscous drag, and hence Reynolds similarity, might be important. As will be seen when bats are addressed Strouhal similarity does apply to bats. If both Reynolds and Strouhal similarity simultaneously apply, then by solving for speed, u, in the definitions of Reynolds and Strouhal numbers, the frequency, f, is seen to be proportional to the inverse of the characteristic length squared , or $f = R\,\nu/St\,\rho l^2$. This sort of dependence of the frequency on the characteristic length was not observed. It should be noted, however, that the characteristic length for viscous drag and that for vortex growth and shedding could be different body dimensions.

Two animals are geometrically similar if one can be made identical to the other by multiplying all its linear dimensions by the same factor (Alexander, 2005). Properties of geometric similarity include surface area, S, being proportional to the square of the characteristic length, l^2, and simultaneously volume, V, being proportional to the cube of the characteristic length, l^3. Since mass, W, is proportional to volume, mass is also proportional to l^3. From equation (3) geometric similarity of the skeletal musculature means that the fundamental propulsion frequency exponent $r = 1.0$. The fundamental frequency constant, c, in equation (3) has the dimension of speed. If the non-skeletal musculature is also geometrically similar with $y = 2/3$, then the entire animal will be geometrically similar.

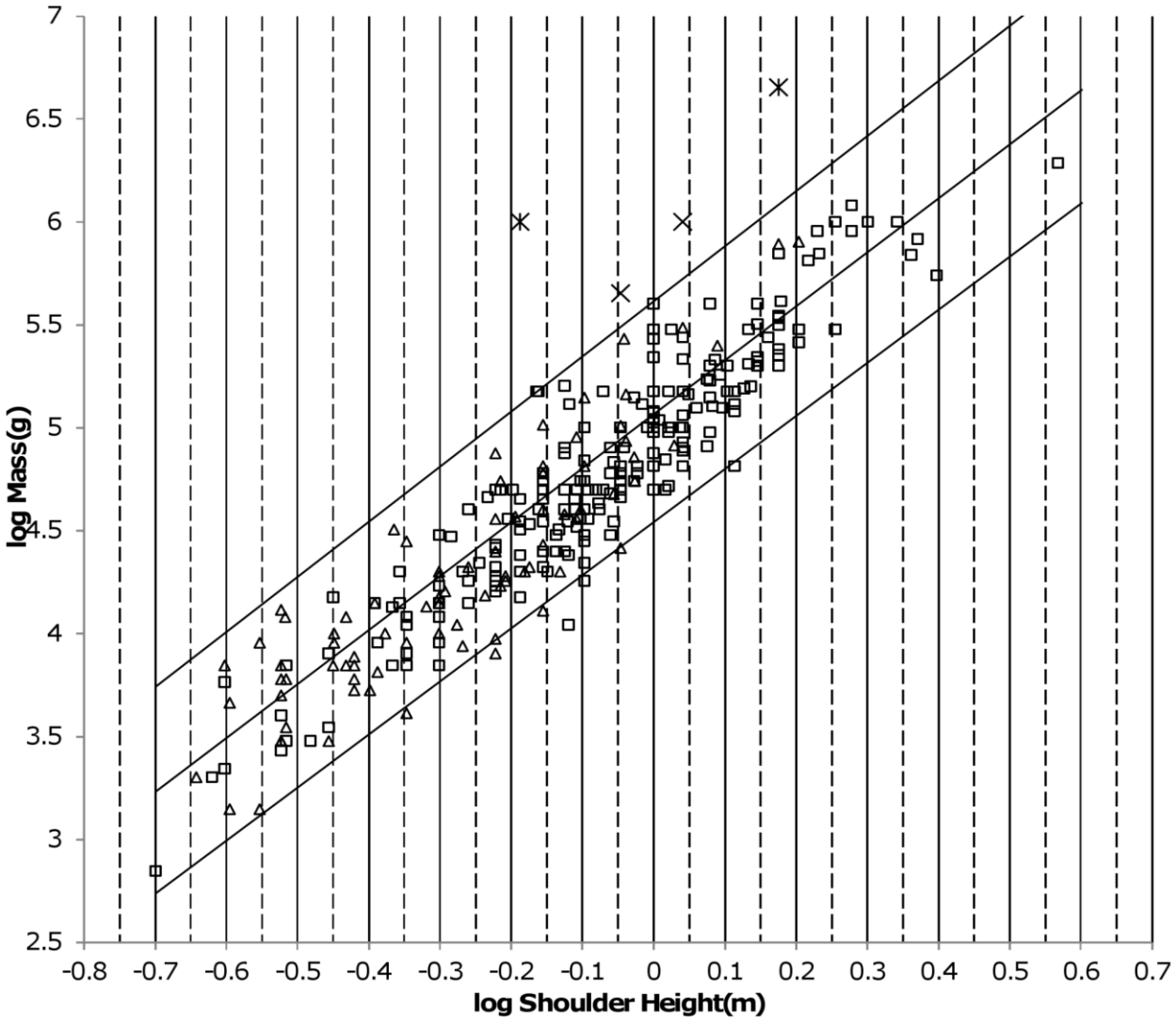

Figure 1. Log body mass as a function of log shoulder height for running/walking Artiodactyla and Carnivora. Data are individual samples from (Nowak, 1999). The upper and lower slanted solid lines are MMLE sturdiness factor boundaries for y = 2/3. The upper boundary was generated with a sturdiness factor, s, of the square root of 3, $(3)^{0.5}$. The lower boundary was generated with s = $(3)^{-0.5}$. The middle slanted line was generated with s = 1.0. The slanted lines are for Froude-Strouhal dynamic similarity. The Artiodactyla mass and shoulder height data are marked by open squares. The Carnivora mass and shoulder height data are marked by open triangles. Excluding *Hippopatamus amphibus* marked by crossed Xes and domestic cattle marked by Xes, R_M^2 = 0.9997. The solid vertical lines demark the AVG method first set of cohorts. The dashed vertical lines demark the second set of cohorts.

Froude and Strouhal dynamic similarity are separately compatible with geometric similarity.

If both Froude and Strouhal similarity simultaneously apply then equating speed in the definitions of the Froude and Strouhal numbers results with the frequency, f, being proportional to the pendulum frequency, $(g/l)^{0.5}$. Substituting this expression for f in equation (1) shows that mass, W, is not proportional to l^3 and thus geometric similarity does not apply.

If only one or the other of the dynamic similarities apply without geometric similarity, there is no particular constraint on the fundamental frequency of propulsion, f. Consequently there is no particular constraint on the exponent r in equation (3).

From equations (2) and (3) geometric similarity means that BMR is proportional to body mass raised to the 2/3 power, $W^{2/3}$. Simultaneous Froude and Strouhal similarity implies that BMR is proportional to body mass raised to a power greater than 2/3. If only one or the other of the dynamic similarities apply without geometric similarity, BMR could be proportional to body mass raised to a range of powers.

Hereafter, when it is stated that geometric similarity applies it also means that either Froude or Strouhal dynamic similarity also applies.

Examining body mass and BMR from the skeletal length perspective rather than from the body mass perspective lead to the concept of the sturdiness factor. The sturdiness factor is a most important concept of MMLE theory. Because of its importance this summary of MMLE theory will conclude with a discussion of the sturdiness factor and some of its more significant properties.

The sturdiness factor is best understood by looking at Fig.1. Figure1 plots 314 samples of log body mass versus log shoulder height for running/walking mammals from the orders Artiocactyla and Carnivora obtained from (Nowak, 1999). Shoulder height is a good surrogate for characteristic length for running/walking mammals as will be discussed in a subsequent section. Three slanting lines are also plotted. The middle line plots equation (3) with the sturdiness factor set to 1.0. The upper line plots equation (3) with the sturdiness factor set to the square root of 3, $(3)^{0.5}$. The lower line plots equation (3) with the sturdiness factor set to $(3)^{-0.5}$. Excluding *Hippopatamus amphibus* and domestic cattle, over 97% of the data are contained between the upper and lower slanting lines.

The data bordering the upper line are for sturdy animals such as a large wolverine (*Gulo gulo*) with a mass of W = 32 kilo grams (kg), characteristic length of l = 0.432 meters (m) and sturdiness factor s = 1.52; a large American black bear (*Ursus americanus*) with W = 270 kg, l = 0.91 m and s = 1.63; a large water chevrotain (*Hyemoschus aquaticus*) with W = 15 kg, l = 0.355 m and s = 1.35; and a small common eland (*Taurotragus oryx*) with W = 400 kg, l = 1.0 m and s = 1.73;. The data bordering the lower line is for gracile animals such as a small bob cat (*Felis rufus*) with W = 4.1 kg, l = 0.45 m and s = 0.556; a large maned wolf (*Chrysocyon*

brachyurus) with W = 26 kg, l = 0.9 m and s =0.568; a small duiker (*Cephalophus monticola*) with W = 3.5 kg, l= 0.35 m and s = 0.70; and a large roe deer (*Capreolus pygargus)* with W = 50 kg, l = 1.0 m and s = 0.687. At the same characteristic length an animal with a greater sturdiness factor is more massive than an animal with a lesser sturdiness factor - hence the nomenclature 'sturdiness' factor.

The sturdiness factor adds additional information about the physique of an animal that is missing from relationships of the form aW^b. At the same characteristic length, an animal with a greater sturdiness factor has more skeletal muscle and non-skeletal muscle mass and hence more mitochondria. Its BMR should be greater than that of a less sturdy animal as is reflected by equation (2).

MMLE theory considers the sturdiness factor to be a random variable approximately uniformly distributed between an upper boundary and a lower boundary with a mean value of 1.0. As will be shown later in the current paper a sturdiness factor of $(3)^{0.5}$ for the upper and $(3)^{-0.5}$ for the lower boundary works for running/walking placental mammals, rodents and bats.

Methods. Determining numerical values for the universal constants G_m, G_o and G_r requires three equations. Since equation (3) is just a version of equation (1) another equation is required. Numerical values for the constants G_m and G_o could be obtained by solving equation (3) for two different samples of body mass and characteristic length l. MMLE uses a more general approach.

An approximation to equations (1) and (3) is:

$$W = dl^x \qquad (4)$$

This expression is useful for establishing the approximate relationship between body mass, W, and characteristic length, l, by regression analysis of W, l data for a group of animals. For least squares regression a figure of merit for how well the expression represents the data is the coefficient of determination, R^2. The coefficient of determination measures the fraction of the dependent variable's variance that is explained by the expression.

Least squares regression is performed on the logarithmic version of equation (4), log(W) = log(d) + xlog(l), to obtain best estimate values for log(d) and x.

Another useful expression is obtained by equating the derivatives with respect to log(l) of the logarithms of equations (3) and (4) to obtain, for s = 1.0 and geometrically similar non-skeletal musculature where y = 2/3, an equation for the exponent x in equation (4):

$$x = 2.0 + r + (1-r)(G_o/e)^{3/2}/(l^{(r-1)}G_m/kec + (G_o/e)^{3/2}) \qquad (5)$$

Equation (5) is the third equation needed to establish numerical values for the universal constants G_m, G_o and G_r.

Two types of least squares regression were used: Phylogenetically Informed (PI) Generalized Least Squares and a type that is unique to MMLE theory that is named "AVG regression" in this paper. The PI Generalized Least Squares regression analyses were conducted using the BayesTraits computer program (Pagel, Meade & Barker, 2004). PI methods are used to control for the lack of statistical independence among species (Freckleton, Harvey & Pagel, 2002). AVG regression is explained later in this section.

It is emphasized that the regression analyses were primarily used to estimate the parameters that occur in equations (2) and (3).

The Microsoft Windows version of BayesTraits together with the companion programs BayesTrees and BayesTreesConverter available at www.evolution.rdg.ac.uk were used.

BayesTraits requires phylogenetic trees. For all mammals except Carnivora the tree for all mammals was used that is available as supplemental information from the online version of (Fritz, Bininda-Emonds & Purvis, 2009) at http://onlinelibrary.wiley.com/doi/10.1111/j.1461-0248.2009.01307.x/suppinfo .This tree contains 5020 species of mammals. For Carnivora an updated tree was used that is available from the online version of (Nyakatura & Bininda-Emonds, 2013)at www.ncbi.nlm.nih.gov/pmc/articles/PMC3307490/ . This tree contains 286 Carnivore species. The trees were converted to nexus format input for BayesTraits using BayesTrees Converter. They were then pruned to the species that were contained in the data sets that were being analyzed using BayesTrees and manual editing of the nexus files. For running/walking mammals the updated pruned Carnivora trees were grafted to the older trees that had been pruned to the Artiodactyla, Proboscidae and Perissodactyla species that were contained in the data sets. Polytomies were automatically resolved using the BayesTrees resolve trees command with a branch length of 0.01 million years.

The PI regression analyses were performed with the BayesTraits continuous regression model and the maximum likelihood analysis type. The inputs were set to estimate the parameter lambda.

Lambda is found by maximum likelihood. It usually varies between 0.0 and 1.0. It is a multiplier of the off-diagonal elements of the Generalized Least Squares variance-covariance matrix. Lambda = 0.0 indicates evolution of traits that is independent of phylogeny, while lambda = 1.0 indicates that traits are evolving according to Brownian motion. Intermediate values indicate that traits have evolved according to a process in which the effect of phylogeny is weaker than in the Brownian model (Pagel, 1999; Freckleton, Harvey & Pagel, 2002; Pagel, Meade & Barker, 2004; Capellini, Venditti & Barton, 2010). BayesTraits results generated with lambda = 0.0 are the same as those obtained with Ordinary Least Squares (OLS) linear regression. Results generated with lambda = 1.0 are the same as those generated by phylogenetically independent contrasts (Capellini, Venditti & Barton, 2010). Occasionally lambda was estimated to be greater than 1.0.

This can be interpreted as traits that are more similar than what is predicted by Brownian motion (Freckleton, Harvey & Pagel, 2002).

The BMR, body mass data from (Kozlowski, Konarzewski & Gawelczyk, 2003) is species-averaged in which a datum is an average of the measurements of all individuals from the same species. The body mass, characteristic length data from (Nowak, 1999) are mostly maximum and minimum measurements of individuals from the same species or genera in which a datum is the measurements for the largest or smallest individual measured in the taxon. BayesTraits is compatible with species-averaged data. BMR, body mass data were inputted directly. Body mass, characteristic length data were taxon-averaged before being inputted to BayesTraits.

By equation (3) MMLE predicts the absolute value of body mass of individual animals rather than taxon-averaged values. The AVG regression method is compatible with individual animal data such as the unmodified data from (Nowak, 1999).

AVG regression is best explained with reference to Fig. 1. The appendix to the original paper shows that the OLS regression relationship between body mass and characteristic length is given by the equivalent of equation (3) evaluated with a sturdiness factor value of s = 1.0 for a MMLE phylogenetically homogeneous group. A MMLE phylogenetically homogeneous group is a group of animals for which the only parameters in equation (3) that differ between individuals are the characteristic length, l, and the sturdiness factor, s. The s = 1.0 regression relationship is plotted by the middle slanting line in Fig. 1. For any particular characteristic length, the mean of the logs of all body masses with that characteristic length that are uniformly distributed between the upper and lower sturdiness factor boundaries is the log of the body mass predicted by equation (3) evaluated with a sturdiness factor of s = 1.0. MMLE takes advantage of this property to get linear regression relationships between log body mass regressed on log characteristic length with coefficients of determination, R^2, that are very nearly 1.0.

The method is to group the body mass and characteristic length data into adjacent but non-overlapping cohorts. Each cohort is bounded by a lower and upper value of characteristic length. For the running/walking Artiodactyl and Carnivore data of Fig. 1, a set of 13 cohorts was selected so that they would be evenly spaced on the log characteristic length axis. The solid vertical lines in Fig. 1 show the boundaries of the cohorts. Within each cohort the characteristic lengths for the data contained in the cohort was linearly averaged to get a single value for the cohort. The body masses contained in the cohort were also linearly averaged to get a single value for the cohort. As a check for reasonableness a second set of cohorts was used. Each of these second cohorts overlapped the lower and upper length halves of adjacent cohorts from the first set of cohorts. The dashed vertical lines in Fig. 1 show the boundaries of the second cohorts. Because of the overlapping there are 14 second cohorts in Fig. 1. The mass and length data in the second cohorts was treated in the same way as it was in the first cohorts. An OLS linear regression was then performed using the logarithms of the cohort average mass and average length as data for both the first and second cohort sets. The regression relationship that was

obtained for the Fig. 1 first cohort set was log(W) = 2.4861log(l) + 5.03 with R^2 = 0.9911. The relationship obtained for the second set was log(W) = 2.6076log(l) + 5.01 with R^2 = 0.9784.

The slopes of the two relationships differed significantly. This indicated that the slopes of the regression relationships were not very reasonable estimates of the exponent x in equations (4) and (5). A look at Fig. 1 indicates why the slopes could be so different. The average number of samples per first cohort is 23.7. The lowest characteristic length first cohort only contains six samples. The two upper most characteristic length first cohorts only contain one sample. Combining these sparsely populated first cohorts with their next adjacent cohort results in a first cohort regression relationship of log(W) = 2.6207log(l) + 5.0557 with R^2 = 0.9932. For the second set of cohorts, the lowest characteristic length cohort only contains one sample. The three upper most characteristic length cohorts only contain four samples. Combining these sparsely populated second cohorts with their next adjacent cohort results in a second cohort regression relationship of log(W) = 2.604log(l) + 5.0611 with R^2 = 0.9933. The slopes of these relationships are much closer than are the slopes of the previous relationships and a greater fraction of the variances are explained. Performing a OLS linear regression using both the first and second cohort data as a way of averaging the two cohort sets yields log(W) = 2.6112log(l) + 5.0584 with R^2 = 0.9932. This regression of the combined cohort data is arbitrarily designated an "AVG" regression in the present paper. The slope of this AVG relationship was taken to be a good estimate of the exponent x in equations (4) and (5).

Combining sparsely populated cohorts into a cohort with a population that more closely approaches the average cohort population density finds some justification in the MMLE proposition that sturdiness factor is uniformly distributed between upper and lower sturdiness factor boundaries. A cohort needs a sufficient number of samples so that its mean is most likely close to the theoretical mean that would be obtained with a very large number of samples.

The PI regression relationships are helpful for partitioning populations into MMLE phylogenetically homogeneous groups to which the AVG regression technique can be applied as when a geometrically similar partition can be identified by a log(mass) regressed on log(length) slope of 3.0 or a log(BMR) regressed on log(mass) slope of 2/3. Since the only parameters in equation (3) that differ between individual members of a MMLE phylogenetically homogeneous group are the characteristic length, l, and the sturdiness factor, s, further consideration of the relatedness of members is not necessary.

Regression analysis measures the error for a datum as the distance between the datum and a line established by the regression analysis. The line minimizes the sum of the squares of the errors. Using Fig. 1 as an example, the usual way of measuring error for a datum is the vertical distance from the datum to the middle slanting line given by equation (3) evaluated with a sturdiness factor s = 1.0. The coefficient of determination, R^2, equals 1.0 – (sum of the squares of the errors)/(variance of the dependent variable). R^2 is interpreted as the fraction of the dependent

variable variance that is explained by the regression line (Edwards, 1984). The dependent variable in Fig. 1 is body mass.

In MMLE theory the OLS regression line can be replaced by a 'regression band'. The band is the area enclosed by the sturdiness factor boundaries. Recognizing this fact, R^2 can be replaced by an MMLE version that is denoted "R_M^2". R_M^2 is computed in the same ways as R^2 except that the error for a datum that falls between the sturdiness factor boundaries is zero and the error for a datum that that falls outside the sturdiness factor boundaries is the distance between the datum and the nearest sturdiness factor boundary. $R_M^2 = 0.9997$ for the data in Fig. 1.

R_M^2 is very nearly unity because the data considered in the present paper mostly lies between the sturdiness factor boundaries or very near to a boundary. Coverage, R, which is the fraction of the data that lies between the boundaries, is another figure of merit that is usually smaller than R_M^2.

Equation (3) evaluated with correct sturdiness factors exactly predicts every datum obtained from (Nowak, 1999) that is shown in Fig. 1. There is no unexplained variance. R_M^2 is interpreted as a measure of how well data clusters within the sturdiness factor boundaries. R_M^2 is useful for estimating values for the parameters that appear in equation (3) when they may differ from the values established for running/walking placental mammals.

By examining individual animal metabolic rates and masses, (Hudson, Isaac &, Reuman, 2013) recently reported substantial metabolic rate heterogeneity at the species level and commented that this is a fact that cannot be revealed by species-averaged data sets. It was further commented that individual data might be more important than species-averaged data in determining the outcome of ecological interactions and hence selection. Heterogeneity is predicted by equations (2) and (3) due to variation of characteristic length and sturdiness factor among the individuals composing a species. The AVG regression method is compatible with species level heterogeneity.

However, assuming that there is an individual within a taxon whose body mass and characteristic length are equal to the taxon-averaged values, R_M^2 can be applied to taxon-averaged data.

Thus sturdiness factor boundaries and R_M^2 can also be applied to the BMR, body mass data from (Kolokotrones et al, 2010). The boundaries are calculated by using equation (3) with the bounding sturdiness factors to calculate the body mass and using equation (2) with the bounding sturdiness factors to calculate the BMR for characteristic lengths that span the range of interest. The associated value of R_M^2 can then computed using the BMR as a function of body mass boundaries.

Equations (2) and (3) evaluated with a correct sturdiness factor and characteristic length exactly predicts every BMR and body mass datum used in the present paper that was obtained from (Kolokotrones et al, 2010). There is no unexplained variance.

As will be discussed later the ability of equation (3) to exactly predict every datum extracted from one data set and its ability, when combined with equation (2), to exactly predict every datum extracted from another data set does not necessarily mean that there is no unexplained variance with MMLE theory.

The calculated numerical values reported in the present paper are given with four significant digits to the right of the decimal point. It is suspected that the data used is not accurate enough to support this precision.

Running/Walking Placental Mammals. The original paper established the numerical values for the constants in the MMLE equations by analysis of the running/walking members of the orders Artiodactyla, Carnivora, Perrisodactyla and Proboscidae. The fundamental frequency of propulsion was established as the pendulum frequency obtained when both Froude and Strouhal dynamic similarity apply simultaneously.

Limb length was considered to be the characteristic length that establishes the pendulum frequency. (Raichlen, Pontzer & Shapiro, 2013) find that hip joint to limb center of mass is a better length for establishing the pendulum frequency. However little limb length or hip joint to limb center of mass data was available. Shoulder height data was more available, so shoulder height was adopted as an approximation of the characteristic length, l. 163 individual shoulder height, body mass samples were obtained from (Walker, 1968). The data was analyzed using the AVG regression method. The result was the relationship log mass = 2.66 log(shoulder height) + 2.17 with a correlation coefficient = 0.993. Thus the slope, x, in equation (5) was 2.66. Body mass was about 75 kg at the logarithmic mean shoulder height of the data of 0.782m. These values were used in the equivalent of equations (3) and (5) with unity sturdiness factor and unity mitochondrion capability quotient to simultaneously solve for the constants G_m/k and G_o that occur in the equations. The results were $G_m/k = 295000$ g/m^2 sec and $G_o = 1353$ g$^{0.667}$/m^2 in the units used in the present paper. By examining the graph of body mass as a function shoulder height for the 163 samples, it was estimated that mass as a function of shoulder height lines computed from equation (3) with sturdiness factor values of the square root of 3, $(3)^{0.5}$, and its inverse, $(3)^{-0.5}$, approximately bounded the data.

BMR was predicted to scale as body mass raised to the 2/x power. Since x = 2.66 this meant that BMR scaled as body mass raised to the 0.75 power in agreement with Kleiber's law. Kleiber's law with additional data from (Economos, 1982) was used to estimate the constant G_r in equation (2) to be 142 watts/m^2.

An expanded version of the methodology in the original paper was used to determine the constants in equations (1), (2) and (3) in the present paper. AVG and PI regressions of the new body mass on shoulder height data were used to determine the exponent in equation (4). This regression relationship was then to be used to determined body mass at a 'middle' shoulder height. Then equations (3) and (5) were solved simultaneously for the constants G_m/k and G_o

occurring in the equations using unity sturdiness factor and unity mitochondrion capability quotient. The method for determining the constant G_r in equation (2) was more complicated.

226 individual and 129 species-averaged mass and shoulder height samples were obtained from (Nowak, 1999) for Artiodactyla (Data S1). *Hippopotamus amphibius* and *Bos Taurus* (aurochs and domestic cattle) were excluded from the analysis. *H. amphibious* was excluded because it is amphibious with significant adaptations for an aquatic existence. Aurochs were excluded because they are extinct. Domestic cattle were excluded because they have been bred for human utility rather than survival in nature. Figure 1 shows that both species are outliers to the main sequence of mass and shoulder height data for Artiodactlya. With these exceptions, the data spans the Artiodactyla range of mass and shoulder height from a small Asiatic mouse deer (*Tragulus javincus*) with a mass of 700g and shoulder height of 0.2m to a large giraffe (*Giraffa camelopardalis*)with a mass of 1930000g and a shoulder height of 3.7m.

84 individual and 43 species-averaged mass and shoulder height samples were obtained from (Nowak, 1999) for Carnivora (Data S1). The Mustelidae were mostly excluded because shoulder height was not given except for wolverines (*Gulo gulo*) and honey badgers (*Mellivoracapensis*). Shoulder height was not given for most of the smaller Carnivora so that the smallest sample was a raccoon (*Procyon*) with a mass of 2000g and a shoulder height of 0.228m. Thus while nearly three orders of magnitude of mass from the small raccoon to a large polar bear (*Urus martimus*) at 800000g are included in the data, almost two orders of magnitude of mass from a small least weasel (*Mustela nivalis*) at 30 g to the small raccoon were not available.

Table 1 shows the AVG and PI regression analysis results obtained with this data. From the Artiodactyla + Carnivora AVG mass on shoulder height regression the exponent, x, for equation (4) is 2.61.Since total body mass scales with an exponent, 2.61, that is greater than the exponent with which the skeletal muscule mass scales, 2.5, the non-skeletal muscle mass must scale with an exponent greater than 2.61. The simplest assumption is geometric similarity so that the non-skeletal muscle mass scales with an exponent of 3.0. The corresponding value for y is 2/3. The shoulder height is 0.86m for the mid point of the Artiodactyla + Carnivora log(shoulder height) data. By the AVG regression relationship the associated body mass is 77155g. Simultaneously solving equations (4) and (5) with these values results in $G_m/k = 274000\ g/m^2$ sec and $G_o = 900\ g^{0.667}/m^2$.

The PI mass on shoulder height regression slope for Artiodactyla + Carnivora is not significantly different from 2.5 as the log likelihood ratio for the table 1 slope and 2.5 is less than 4.0 (Pagel, 1999). Since for Froude-Strouhal similarity the skeletal musculature scales with an exponent of 2.5, this implies that the non-skeletal musculature also scales with an exponent of 2.5 which means that y = 0.8 in equation (3). The equivalent of equation (5) with y = 0.8 and r = 0.5 only states that x = 2.5 and provides no information for estimating G_m/k and G_o. Additionally equation (3) must be used to estimate the dimensionality factor, m.

G_m/k should not change if y changes. The shoulder height is 0.88m for the mid point of the Artiodactyla + Carnivora log(shoulder height) data. By the PI regression relationship the associated body mass is 86538g. Using the previously established values of G_m/k and G_o with y = 0.8 in equation (3) evaluated at these shoulder height and body mass values results with a values for the dimensionality factor of m = 4.425 $g^{0.133}$.

Table 1. Results of regression analyses for running/walking placental mammals.

Order or Family	Regression Type	Independent Variable	Dependent Variable	Slope	Intercept	R^2	Number Samples
Artiodactyla + Carnivora	AVG	Height(m)	Mass(g)	2.6112	5.0584	0.9932	NA
	PI(0.89)	Height(m)	Mass(g)	2.4893	5.076	0.8435	172
All	AVG	Height(m)	Mass(g)	2.8711	5.1677	0.9886	NA
	PI(0.92)	Height(m)	Mass(g)	2.4875	5.2517	0.8424	189
Ruminant Artiodactyla	PI(0.0)	Mass(g)	BMR(watts)	0.7805	-1.8058	0.9742	19
Carnivora	PI((0.87)	Mass(g)	BMR(watts)	0.7579	-1.8826	0.909	59
Carnivora less Mustelidae	PI(0.61)	Mass(g)	BMR(watts)	0.758	-1.8937	0.9053	46
Mustelidae less Enhydra	PI(1.0)	Mass(g)	BMR(watts)	0.6852	-1.4688	0.9653	12
Perrisodactyla+Proboscidae	AVG*	Height(m)	Mass(g)	2.26	5.54	0.93	NA
	AVG**	Height(m)	Mass(g)	2.59	5.44	0.96	NA
	PI(1.02)	Height(m)	Mass(g)	1.376	5.716	0.9442	17

The regression expressions are: Log(dependent variable) = slope X log(independent variable) + intercept. AVG means the cohort averaging regression method. PI(n) means the phylogenetic informed regression method using BayesTraits and the number in parentheses is the estimated value of lambda. "All" in the Order or Family column means the combination of Artiodactyla, Carnivora, Perissodactyla and Proboscidae. Height(m) is shoulder height in meters. Mass(g) is body mass in grams. BMR(watts) is basal metabolic rate in watts. NA means Not Applicable. *, AVG method first set of cohorts values; **, AVG method second set of cohorts values.

The new values for G_m/k and G_o are less than the values computed in the original paper. The 163 samples in the original paper included two Probicidae and 11 Perissodactyla whereas the 310 samples in the present paper were entirely Artiodactyla or Carnivora.

Figure 2 shows the MMLE mass as a function of shoulder height sturdiness factor boundaries for simultaneous Froude-Strouhal dynamic similarity as predicted by equation (3) evaluated with the new values for G_m/k and G_o for both y = 2/3 and for y = 0.8 with the corresponding values of the dimensionality factor, m. The upper boundary uses a sturdiness factor of $(3)^{0.5}$. The lower boundary uses a sturdiness factor of $(3)^{-0.5}$. The reference (Nowak, 1999) mass and shoulder height samples for Artiodactyla and Carnivora are also shown. The data spans this full range of sturdiness factor for both values of y. The boundaries are hardly distinguishable for the two y values.

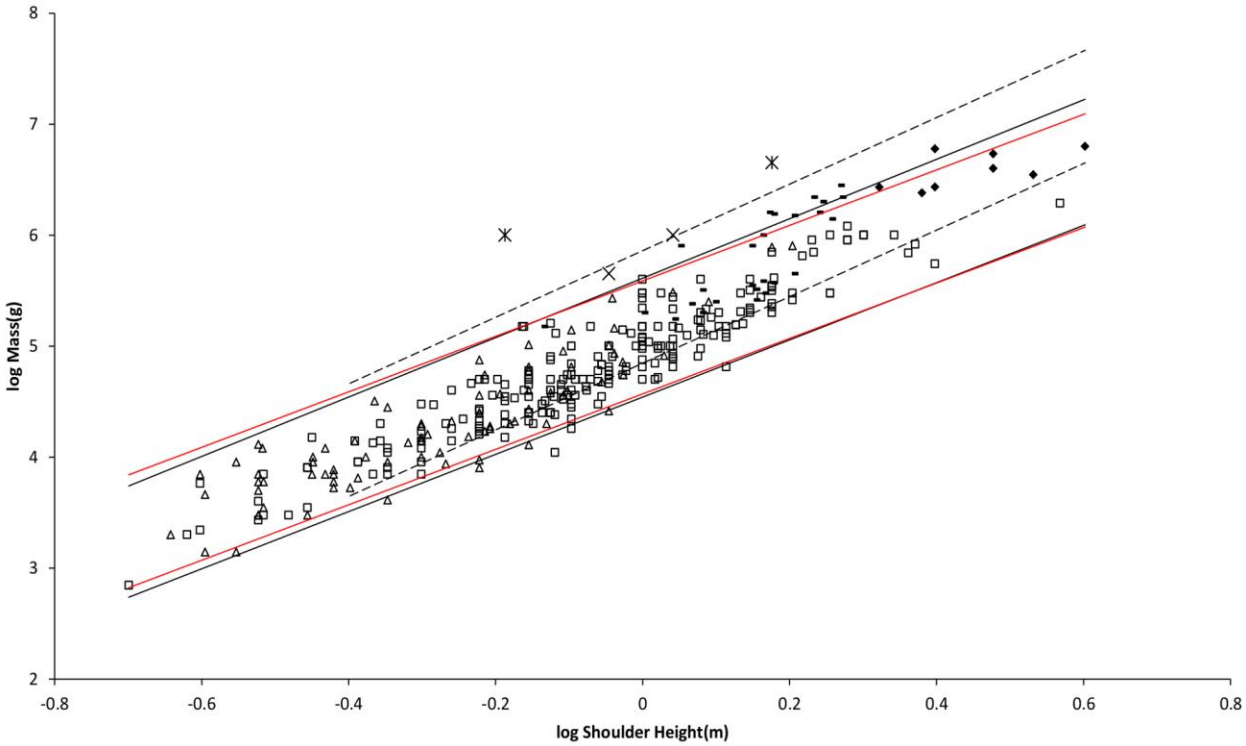

Figure 2. Log body mass as a function of log shoulder height for running/walking placental mammals. Data are individual samples from (Nowak, 1999). The solid and dashed lines are MMLE sturdiness factor boundaries. The upper boundaries were generated with a sturdiness factor $s = (3)^{0.5}$. The lower boundaries were generated with $s = (3)^{-0.5}$. The solid boundary lines are for Froude-Strouhal dynamic similarity. The black solid lines are for y = 2/3. The colored solid lines are for y = 0.8. The dashed boundary lines are for geometric similarity. The colored boundary lines, the geometric similarity boundary lines and the Perissodactyla and Proboscidae mass, shoulder height data have been added to the Artiodactyla and Carnivora data displayed in figure 1. For Artiodactyla and Carnivora $R_M^2 = 0.9997$ with respect to the solid black boundaries and $R_M^2 = 0.9992$ with respect to the colored boundaries. For Perissodactyla and Proboscidae $R_M^2 = 1.0$ with respect to the geometric similarity boundaries. Perissodactyla data are marked with solid rectangles. Proboscidea data are marked with solid diamonds. Aritiodactyla data are marked with open squares. Carnivora data are marked with open triangles. Crossed Xes mark *Hippopotamus amphibious*. Xes mark domestic cattle.

26 individual and 14 species-averaged mass and shoulder height samples were obtained from (Nowak, 1999) for Perissodactyla. Eight individual and three species-averaged samples were obtained for Proboscidae (Data S1). Table 1 shows the AVG and PI regression analysis results obtained with this data. The first set of cohorts and the second set of cohorts regression relationships for Perissodactyla and Proboscidae combined differed enough to make the AVG analysis suspect and the slope of the PI relationship is very different from the other relationship's slopes. Both the y = 2/3 and the y = 0.8 sturdiness factor boundaries nearly embrace the combination of Artiodactyla, Carnivora, Perissodactyla and Proboscidae, or 'all' runners/walkers, in Fig. 2. A few Proboscidae and Perissiodactyla are outliers. From table 1 the PI regression of body mass on shoulder height indicates that all runners/walkers scale with the same slope as Artiodactyla + Carnivora, albeit with a greater intercept value that would require revision of the constants in equation (3). With a slope of 2.87 the AVG regressions of mass on shoulder height for all runners/walkers indicates a combination of Froude-Strouhal and geometric similarity. A geometrically similar fundamental frequency of 1.4 m/sec divided by shoulder height was heuristically found to embrace the Perissiodactyla and Proboscidae data as shown in Fig. 2. Other than the change to the fundamental frequency formulation, the MMLE geometric similarity sturdiness factor boundaries in Fig. 2 use the same constants that were used to generate the Froude-Strouhal boundaries for y = 2/3. The data very nearly span the full range of sturdiness factor between the boundaries. The relationship between mass and shoulder height for Perissodactyla and Proboscidae may be better explained by geometric similarity.

For running/walking placental mammals the reference (Kolokotrones et al, 2010) BMR and body mass species-averaged data set contained 20 samples for Artiodactyla and 58 samples for Carnivora.

There are doubts that ruminant Artiodactyla can meet the criteria for measuring BMR (McNab, 1997; White & Seymour, 2003). All but one of the Artiodactyla samples were ruminants. For these reasons the BMR and mass data for ruminant Artiodactyla and Carnivora were analyzed separately. Ruminants inability to achieve a post absorptive state should not affect the relationship between body mass and shoulder height so revisiting that analysis because of this issue is not needed.

There is a major composition difference between the mass and shoulder height data and the BMR and mass data for Carnivora. Mustelidae compose only about 1% of the mass and shoulder height data whereas they compose over 20% of the BMR and mass data. For this reason the Mustelidae data was separated from the rest of the Carnivora data as shown in table 1.

The log(shoulder height) mid point of the Carnivora data is l = 0.65m. A carnivore with this shoulder height would have a body mass of 40800g by the PI Artiodactyla + Carnivora mass on shoulder height regression relationship from table 1. Its non-Mustelidae BMR would be 39.9 watts by the PI BMR on mass regression relationship from table1. From equation (2) $G_r = 94.5$ watts/m^2.

Since the coefficient of determination, R^2, for the AVG Artiodactyla + Carnivora mass on shoulder height regression in table 1 is very nearly unity, the expression can be inverted to express shoulder height as a function of body mass. Substituting this expression into equation (2) with the G_m/k and G_o values just determined results with log(BMR) = 0.7659log(W) – 3.8744 + log(G_r). Equating this last expression to the Carnivora less Mustelidae regression expression in table 1 results with $G_r = 95.6W^{-0.0079}$ watts/m^2. Ignoring the mass residual, $G_r = 95.6$ watts/m^2. If the mass residual is not ignored then at the mid point of the log(shoulder height) Carnivora data $G_r = 88$ watts/m^2.

A middle value of $G_r = 95$ watts/m^2 was used to generate the MMLE sturdiness factor boundaries in Fig. 3. As discussed in the summary of the derivation of the MMLE equations, this value of G_r should be the basic value for all non-ruminant placental mammals.

Similarly, values for G_{rR} of 138 watts/m^2 and 144 watts/m^2 are obtained for the Artiodactyla log(shoulder height) mid point of 0.86m. These values for G_{rR} for ruminant Artiodactyla are within three percent of the value for G_r computed in the original paper for all running/walking placental mammals. $G_{rR} = 138$ watts/m^2 was used to generated the MMLE sturdiness factor boundaries in Fig. 3.

An increased mitochondrion capability quotient is not the reason that G_{rR} is greater than G_r. By equation (3) a greater mitochondrion capability quotient would result in a less massive animal for the same characteristic length. Figure 2 shows that both Artiodactyla and Carnivora have similar masses at the same characteristic length. The difference between G_{rR} and G_r is more likely the result of sustained digestive activity by ruminant Artiodactyla (McNab, 1997; White & Seymour, 2003).

Figure 3 shows the MMLE BMR as a function of body mass sturdiness factor boundaries for Froude-Strouhal scaling evaluated with the new values for G_r and G_{rR}. The boundaries were generated by simultaneously using equations (2) and (3). The differences between the y = 2/3 and y = 0.8 curves are due to the different masses predicted by equation (3) for the same characteristic length with the different values of y. In terms of R_M^2 the differences are barely distinguishable. The upper boundaries use a sturdiness factor of $(3)^{0.5}$. The lower boundaries use a sturdiness factor of $(3)^{-0.5}$. The reference (Kolokotrones et al, 2010) BMR and body mass samples for Artiodactyla and Carnivora are also shown. The single Proboscid datum (Savage et al, 2004) is included for reference. Ruminant Artiodactyla do have a BMR that is elevated with respect to Carnivora of the same mass. The single non-ruminant Artiodactyla datum, a dromedary camel (*Camelus dromedaries*), is embraced by the non-Mustelidae Carnivora MMLE boundaries rather than the ruminant boundaries. The data more than spans the full range of sturdiness factor.

Also shown in Fig. 3 is the Mustelidae BMR and mass data. It is better embraced by the ruminant MMLE sturdiness factor boundaries, but Mustidae do not have the digestive features

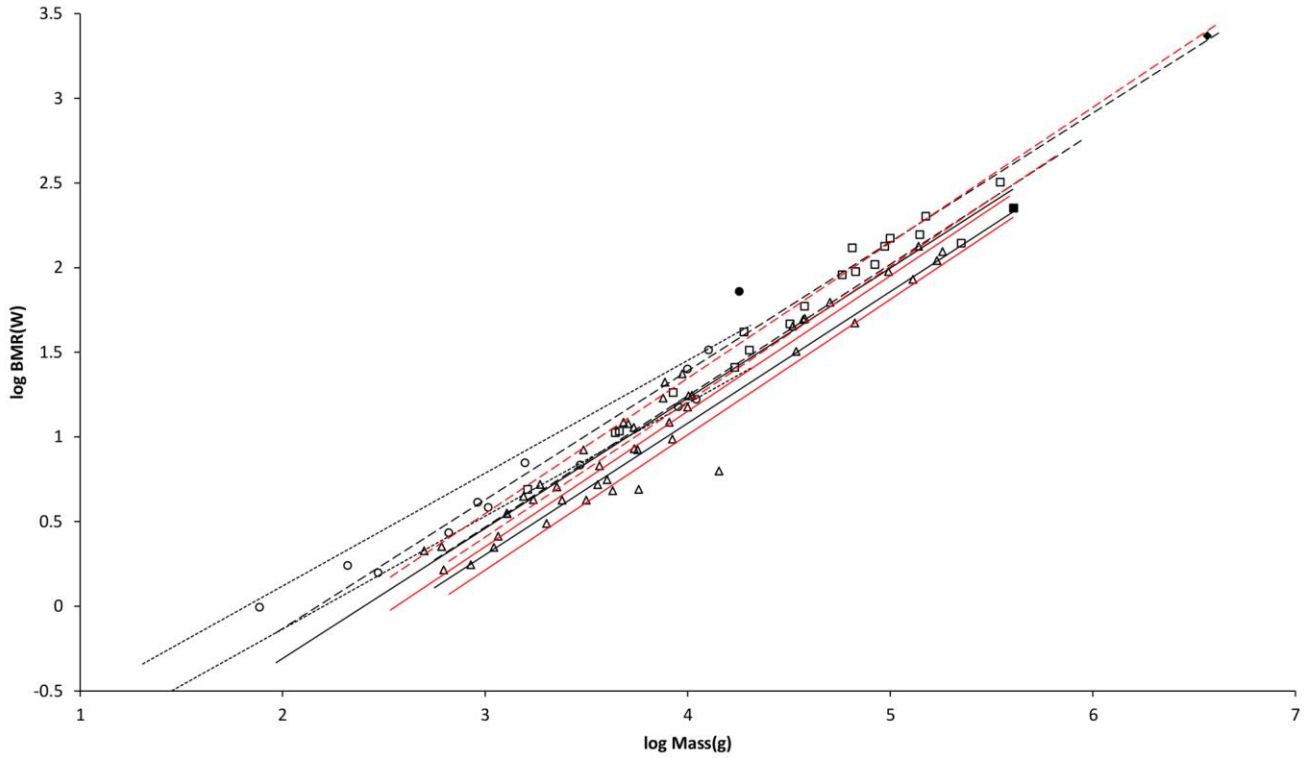

Figure 3. Log BMR as a function of log body mass for running/walking placental mammals. The *Elephas maximus* datum marked by a solid diamond is from (Savage et al, 2004). All other data are species-averages from (Kolokotrones et al, 2010).The solid, dashed and dotted lines are MMLE sturdiness factor boundaries. The upper boundaries were generated with a sturdiness factor $s = (3)^{0.5}$. The lower boundaries were generated with $s = (3)^{-0.5}$. The black lines are for y = 2/3. The colored lines are for y = 0.8. The steeper sloping boundary lines are for Froude-Strouhal dynamic similarity. The shallower sloping boundary lines are for geometric similarity. Ruminant Artiodactyla data are marked by open squares and R_M^2 is 0.9921 with respect to the dashed Froude-Strouhal black boundaries and R_M^2 is 0.9919 with respect to the dashed colored boundaries. *Camelius dromedarius* is a non-ruminant Artiodactyl marked by a solid square. Carnivora less Mustelidae data are marked with open triangles and R_M^2 is 0.9752 with respect to the solid Froude-Strouhal black boundaries and R_M^2 is 0.9655 with respect to the solid colored boundaries. Mustelidae except Enhydra data are marked with open circles and R_M^2 is 0.9999 with respect to the dotted geometric black boundaries. *Enhydra lutris* is an ocean going swimming Mustelid marked by a solid circle.

that are the probable source of the ruminants' elevated BMR. The non-Mustelidae Carnivora value for G_r should apply to the Mustelidae also, but their MMLE boundaries hardly embrace any of the Mustelidae data. Sturdiness factor and characteristic length values could be found so that equations (2) and (3) would exactly predict each Mustelidae BMR and mass datum shown in Fig. 3, but the sturdiness factors would mostly be greater than the maximum needed to predict the BMR and mass for other Carnivore families. Other MMLE parameters can be adjusted so that the Mustelidae data could be bounded by the same sturdiness factor values that bound all the other running/walking placental mammal data.

The Mustelidae data contained one sample for a sea otter (*Enhydra lutris*) which is an ocean going swimmer rather than a runner/walker. Separating this sample from the rest of the Mustelidae data leads to a slope of 0.69 as shown in table 1. This slope is closer to what would be expected for geometric similarity than it is to the Froude-Strouhal similarity slopes for Artiodactyla and Carnivora. Equations (3) with y = 2/3 and a geometric similarity fundamental frequency of 1.4 (m/sec)/l and equation (2) are the MMLE equations for relating BMR to body mass for geometric similarity. Of the constant parameters in these equations, values applicable to Mustelidae for G_m, G_o, and G_r have been established. The MMLE parameters that could be adjusted to account for the Mustelidae BMR deviation are the fundamental propulsion frequency constant, c, the mitochondrion capability quotient, e and the dynamic similarity constant, k. Because many Mustelidae combine swimming with terrestrial locomotion it is possible that their skeletal musculature may not be dynamically similar to other Carnivora and the constant k may be different from a value of 1.0. However, by equation (3), k and c cannot be separated without additional information. The product kc and e were varied to obtain the Mustelidae geometric similarity MMLE sturdiness factor boundaries shown in Fig. 3. Holding constant the combined fundamental propulsion frequency and dynamic similarity constant at a value of kc = 1.4 m/sec as was used for the geometric similarity MMLE mass and shoulder height boundaries for Perissodactyla and Proboscidae required a mitochondrion capability quotient at least 170% of that applicable to other Carnivora. That a Mustelidae mitochondrion would be this much more powerful than other carnivora mitochondria is difficult to believe. Using a combined fundamental propulsion frequency and dynamic similarity constant twice as large as that used for Perissodactyla and Proboscidae reduced the required mitochondrion capability quotient to 130% of that for other Carnivora. An implication would be that more powerful mitochondria allow Mustelidae to move their limbs twice as fast as other placental mammals in performing routine locomotion tasks.

Coverage, R, is the fraction of samples that fall between the MMLE sturdiness boundaries. Separating the Mustelidae from the rest of the Carnivora increased R for the entire Carnivora order from about 0.44 to 0.53 for y = 2/3 and from about 0.39 to 0.49 for y = 0.8. Although coverage is somewhat sparse, many of the samples lie close to the MMLE sturdiness boundaries as the greater R_M^2 values indicate.

MMLE can exactly predict every individual body mass and shoulder height datum from (Nowak, 1999) for running/walking placental mammals that is shown in Fig. 1 and 2. There is no unexplained variance. Once the applicable skeletal muscle similarity is specified and values for the constants G_m and G_o are established, computing an individual animal's mass from its shoulder height only requires specifying its sturdiness factor. Mustelidae are an exception. They require the further specification of a larger mitochondrion capability quotient, e, and an appropriate combined fundamental propulsion frequency and dynamic similarity constants, kc. As shown in Fig. 2 the differences are negligible between y = 2/3 which is indicated by the AVG mass on characteristic length regression relationship and y = 0.8 which is indicated by the PI mass on characteristic length regression relationship. The relationship between mass and characteristic length for Proboscidae and Perissiodactyla may be better explained by geometric similarity.

MMLE also can predict every species-averaged BMR and mass datum from (Kolokotrones et al, 2010) for running/walking placental mammals that are shown in Fig. 3 by using equations (2) and (3) simultaneously. There is no unexplained variance. Body mass is computed with equation (3) as just described. Whether an animal is a ruminant Artiodactyl or not needs to be specified to use the correct value of the constant G_r in equation (2) to compute the animal's BMR from its shoulder height and sturdiness factor. Some iteration of this process may be required if the characteristic length and/or sturdiness factor is not included with the BMR and body mass data for the animal. As shown in Fig. 3 the differences in terms of R_M^2 are negligible between y = 2/3 and y = 0.8.

Rodentia. Rodentia comprise about 20% of families, 39% of genera, and 43% of species of recent mammals. Their masses range over four and a half orders of magnitude and their head and body lengths range over one and a half orders of magnitude (*Mus minutoides* with a mass of 2.5g and head and body lengths of 45mm to *Hydrochaeris hydrochaeris* with a mass of 79,000g and head and body length of 1,300mm). Various species employ scurrying, climbing, gliding, hopping, burrowing, swimming, running/walking , and combinations of these as their primary means of locomotion (Nowak, 1999).

(Nowak, 1999) provides individual data on approximate minimum and maximum masses in grams (g) and head and body lengths in millimeters (mm). The length data are mostly for genera with very little data for species. There is also very little data on shoulder height. Given the available data, linearly relating head and body length to characteristic length was tried. From the reference (Nowak, 1999), 203 individual and 105 taxon-averaged mass, head and body length samples were obtained (Data S2). Reference (Kolokotrones et al, 2010) provides 267 species-averaged BMR in watts (W) and mass in grams (g) samples. Table 2 shows the PI and AVG regression analysis results obtained with this data. The length data was converted to meters (m) for calculations involving equations (1) through (5).

Table 2. Results of Regression Analyses for Rodentia.

Family	Regression Type	Independent Variable	Dependent Variable	Slope	Intercept	R^2	Number Samples
All Rodentia	PI(0.62)	Mass(g)	BMR(watts)	0.7231	-1.7198	0.8968	267
	PI(0.0)	Length(mm)	Mass(g)	2.9482	-4.3637	0.9571	105
	AVG	Length(mm)	Mass(g)	2.8692	-4.1497	0.9956	NA
Non-Cricetidae	PI(0.44)	Mass(g)	BMR(watts)	0.7399	-1.7685	0.9192	176
	PI(0.0)	Length(mm)	Mass(g)	2.9079	-4.2548	0.9571	78
	AVG	Length(mm)	Mass(g)	2.8564	-4.1124	0.9939	NA
Cricetidae	PI(0.55)	Mass(g)	BMR(watts)	0.6597	-1.5408	0.8497	91
	PI(0.0)	Length(mm)	Mass(g)	3.4061	-5.3367	0.9395	27
	AVG	Length(mm)	Mass(g)	2.9531	-4.3561	0.9908	NA

The regression expressions are: Log(dependent variable) = slope X log(independent variable) + intercept. . PI(n) means the phylogenetic informed regression method using BayesTraits and the number in parentheses is the estimated value of lambda. AVG means the cohort averaging regression method. Length(mm) is head and body length in millimeters. Mass(g) is body mass in grams. NA means Not Applicable

Froude similarity should apply to skeletal muscle dynamics in most Rodentia as gravity is the main force affecting their locomotion. This should be true even for swimming as aquatic Rodentia are mainly surface swimmers that experience significant drag through the generation of surface waves in the wake. Drag through the generation of surface waves in the wake is the classic situation to which Froude similarity applies. What should govern the dynamics of burrowing is not clear, but as will be seen Froude similarity seems to work. The mass regressed on head and body length slope for both PI and AVG regressions for all families of Rodentia trends toward the geometric slope of 3.0. The combination of all families except Cricetidae trend toward an intermediate slope between the Froude-Strouhal slope of around 2.55 for mammals the size of Rodentia and the geometric slope. Cricetidae have an AVG mass regressed on length slope nearer the geometric similarity slope and the PI slope exceeds geometric similarity. Cricetidae also have a PI BMR regressed on mass slope that is expected for geometric similarity.

Besides appearing to be more geometrically similar, Cricetidae tend to have a higher BMR when compared to non-Cricetidae of the same mass. For these reasons Cricetidae were analyzed separate from all the other families of Rodentia.

The slope values for mass regressed on head and body mass in table 2 for both PI and AVG regressions are very different from the value of 2.5 obtained for y =0.8 for Artiodactyla + Carnivora. They indicate either geometric similarity with y = 2/3 or a mixture of geometric similarity and Froude-Strouhal similarity with y = 2/3. For non-Cricetidae, the PI regression

slope is not significantly different from the AVG slope as the log likelihood ratio for the two slopes is less than 4.0 (Pagel, 1999). For these reasons y = 2/3 is used in equation (3) for Rodentia.

The characteristic length for Rodentia was assumed to be a constant fraction of head and body length. The fraction's value was estimated by equating the combined Artiodactyla and Carnivora mass regressed on length expression to the all families of Rodentia mass regressed on head and body length for the range of lengths for Rodentia. This results with a fraction that is within the range 0.4 to 0.62 using the PI regression relationship and 0.43 to 0.61 using the AVG relationship. A value of 0.5 was considered to be a reasonable working estimate for this characteristic length scaling fraction.

The characteristic length scaling fraction adds an additional parameter to the number that MMLE uses to predict the absolute values of body mass and BMR. Its addition increases the total number of parameters to 11.

The fundamental locomotion frequency for geometric similarity is a constant divided by the characteristic length. The value of 1.4 m/sec for the constant that worked well for Perissodactyla and Proboscidae was also used as the constant for Rodentia.

Figure 4 shows the MMLE mass as a function of head and body length sturdiness factor boundaries for Froude-Strouhal dynamic similarity and geometric similarity evaluated with these estimates. The reference (Nowak, 1999) mass, head and body length samples for non-Cricetidae Rodentia are also shown.

Figure 5 shows the MMLE BMR as a function of body mass sturdiness factor boundaries for the two similarity regimes. The (Kolokotrones et al, 2010) BMR and mass samples for non-Cricetidae Rodentia are also shown.

Cricetidae were analyzed separate from all the other families of Rodentia because they appear to be more geometrically similar, and they tend to have a higher BMR when compared to non-Cricetidae of the same mass.

As with Mustelidae that have a greater BMR at the same body mass than do other Carnivora, a greater mitochondrion capability quotient would most straight forwardly result in a greater BMR for Cricetidae with the same masses as other Rodentia. This possibility was evaluated for Cricetidae Rodentia. With all other parameters maintained identical to those used for geometrically similar non-Cricetidae Rodentia, the mitochondrion capability quotient was varied until a maximum value of R_M^2 was achieved for both mass as a function of length and BMR as a function of mass. A mitochondrion capability quotient of 1.2 maximized the R_M^2 values. Figure 6 shows the MMLE mass as a function of head and body length sturdiness factor boundaries for geometric similarity evaluated with this mitochondrion capability quotient value. The reference (Nowak, 1999) mass, head and body length samples for Cricetidae Rodentia are also shown.

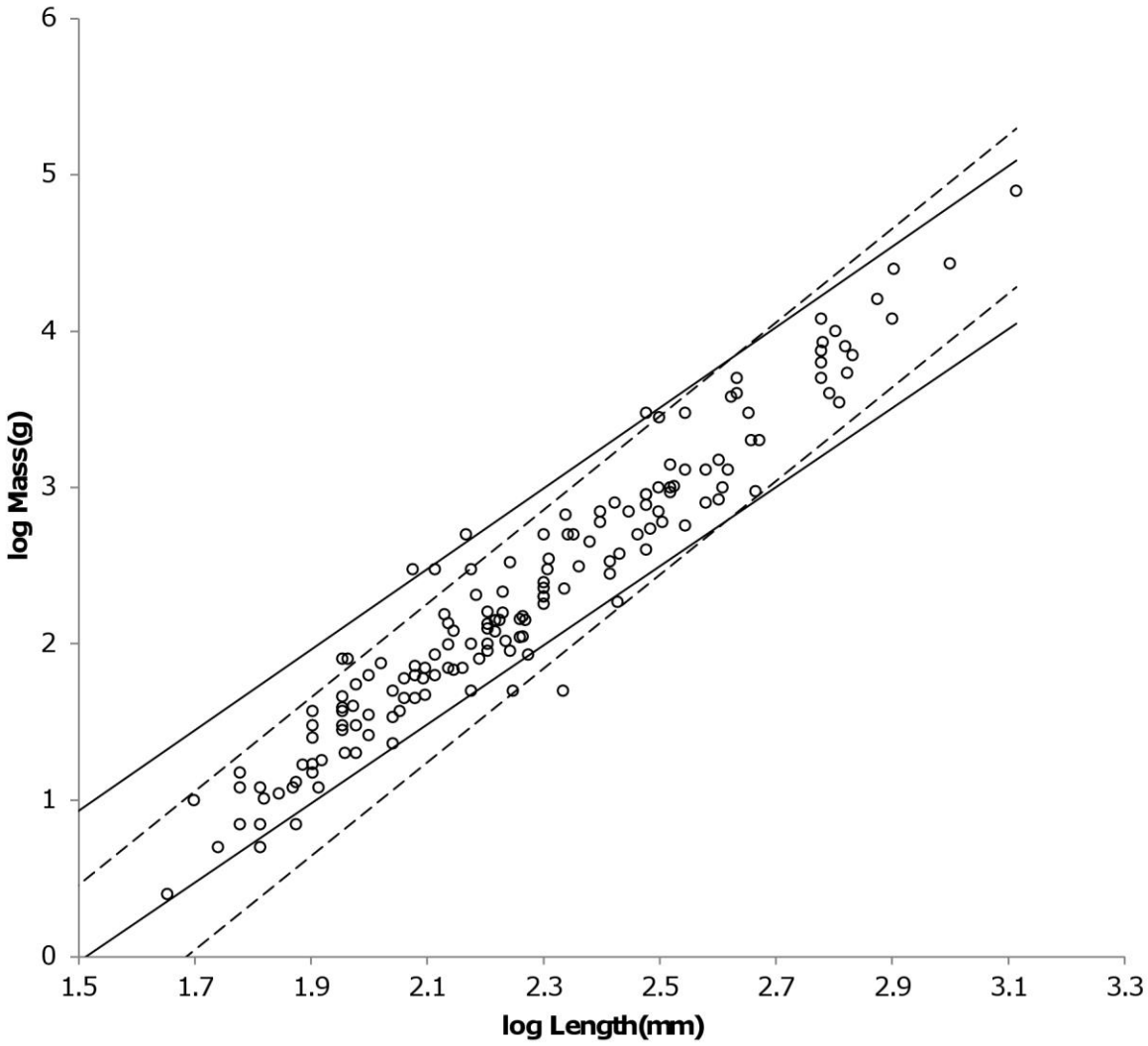

Figure 4. Log body mass as a function of log head and body length for non-Cricetidae Rodentia. Data are from (Nowak, 1999). The solid and dashed lines are MMLE sturdiness factor boundaries. The upper boundaries were generated with a sturdiness factor $s = (3)^{0.5}$. The lower boundaries were generated with $s = (3)^{-0.5}$. The shallower sloping dashed boundary lines are for Froude-Strouhal similarity. The steeper sloping solid boundary lines are for geometric similarity. The non-Cricetidae Rodentia individual mass, head and body length data are marked by open circles. $R_M^2 = 0.9995$ with respect to both sets of boundaries.

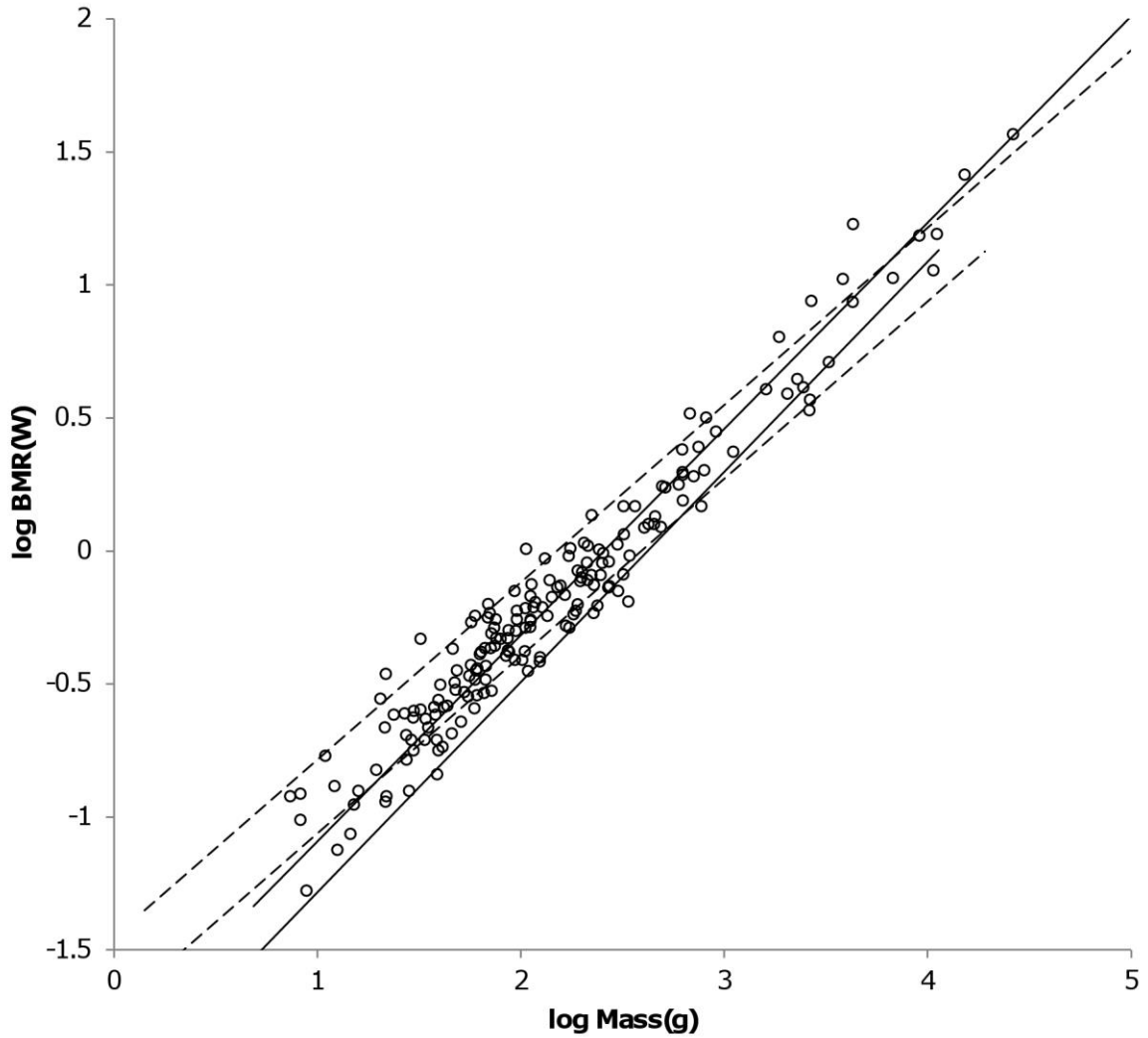

Figure 5. Log BMR as a function of log body mass for non-Cricetidae Rodentia. Data are from (Kolokotrones et al, 2010). The solid and dashed lines are MMLE sturdiness factor boundaries. The upper boundaries were generated with a sturdiness factor $s = (3)^{0.5}$. The lower boundaries were generated with $s = (3)^{-0.5}$. The steeper sloping solid boundary lines are for Froude-Strouhal similarity. The shallower sloping dashed boundary lines are for geometric similarity. The species-averaged non-Cricetidae Rodentia mass, head and body length data are marked by open circles. $R_M^2 = 0.9966$ with respect to both sets of boundaries.

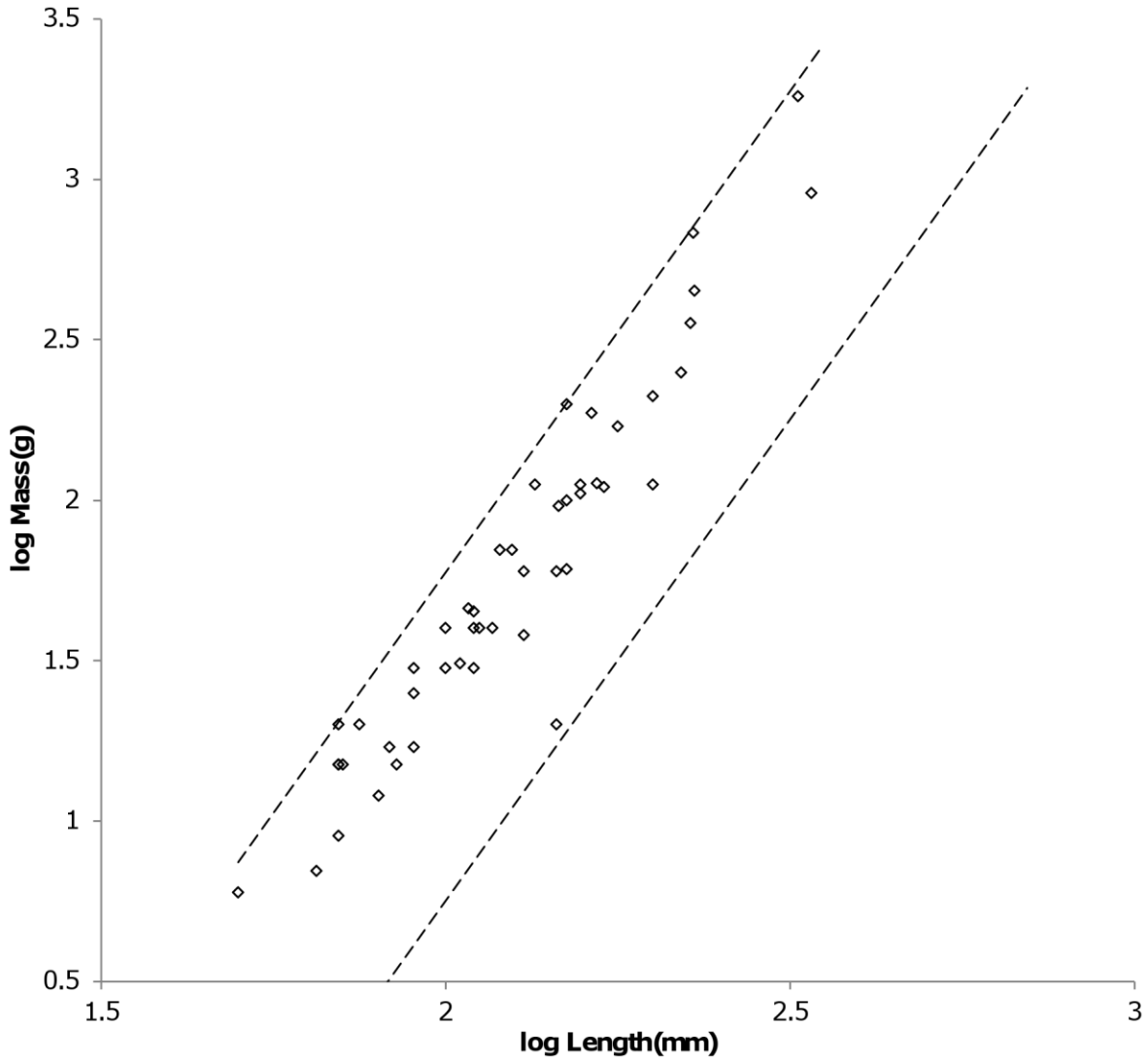

Figure 6. Log body mass as a function of log head and body length for Cricetidae Rodentia. The data are from (Nowak, 1999). The dashed lines are MMLE sturdiness factor boundaries. The upper boundary was generated with a sturdiness factor $s = (3)^{0.5}$. The lower boundary was generated with $s = (3)^{-0.5}$. The boundary lines are for geometric similarity. Cricetidae Rodentia individual mass, head and body length data are marked by open diamonds. $R_M^2 = 1.0$.

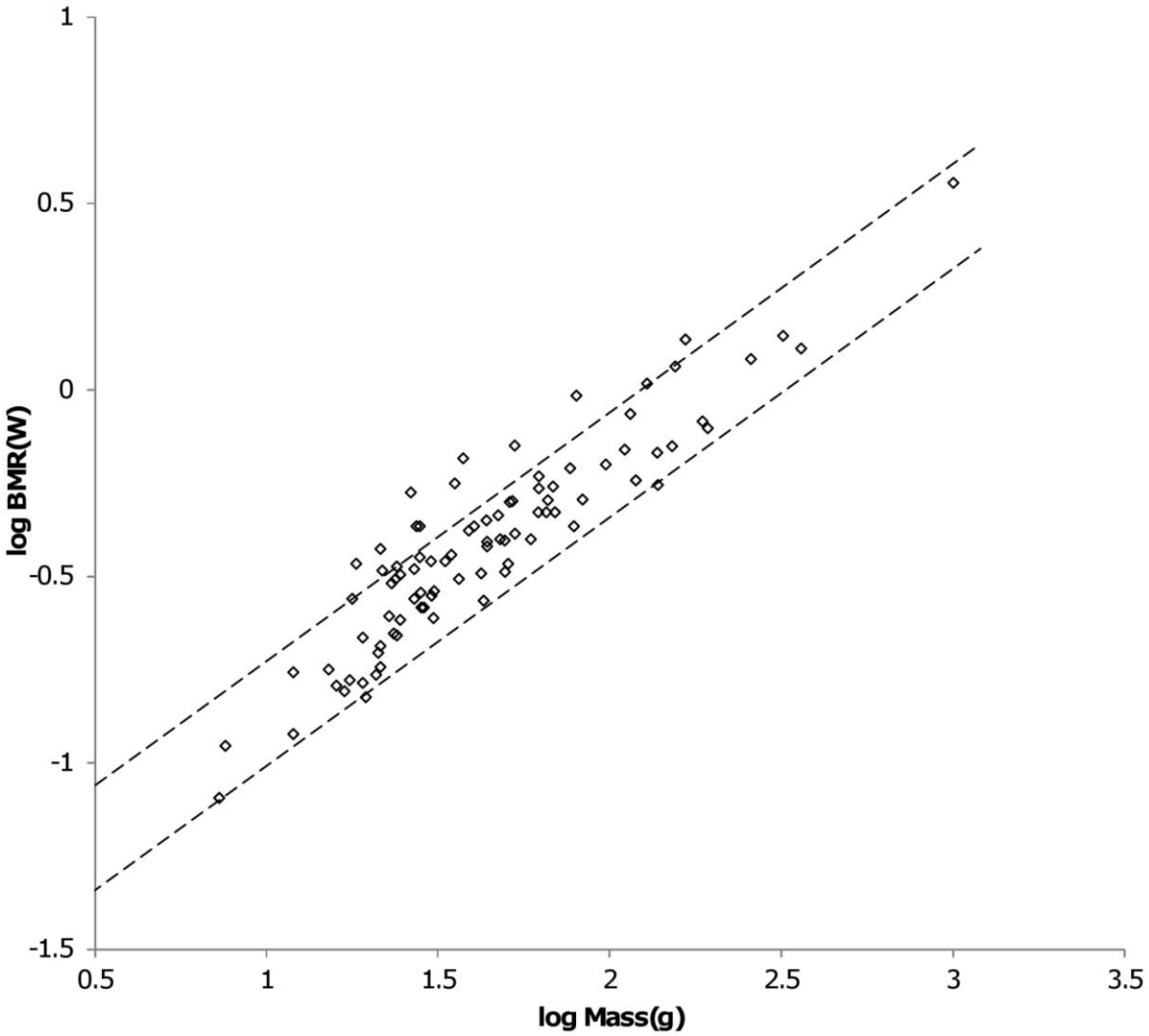

Figure 7. Log BMR as a function of log body mass for Cricetidae Rodentia. The Data are from (Kolokotrones et al, 2010). The dashed lines are MMLE sturdiness factor boundaries. The upper boundary was generated with a sturdiness factor $s = (3)^{0.5}$. The lower boundary was generated with $s = (3)^{-0.5}$. The boundary lines are for geometric similarity. The Cricetidae Rodentia species-averaged BMR, mass data are marked by open diamonds. $R_M^2 = 0.9913$.

Figure 7 shows the MMLE BMR as a function of body mass sturdiness factor boundaries. The reference (Kolokotrones et al, 2010) BMR and mass samples for Cricetidae Rodentia are also shown.

Figure 6 shows that with the exception of a single outlier a tighter range of sturdiness factor for the MMLE boundaries could embrace the Cricetidae mass, head and body length data. The outlier is the larger sample of American harvest mice *(Reithrodontomys)*. However Fig. 7 shows that the full sturdiness factor range is needed to embrace the Cricetidae BMR and mass data.

A mitochondrion capability quotient of 1.2 as an explanation of why Cricetidae have an elevated BMR with respect to other Rodentia is considerably more palatable than the value of this parameter needed to explain the elevated BMR of Mustelidae with respect to other Carnivora.

MMLE can exactly predict every individual body mass, head and body length datum from (Nowak, 1999) for Rodentia that is shown in Fig. 4 and 6. There is no unexplained variance. A characteristic length scaling fraction to translate the available head and body length data to characteristic length gives reasonable results. Then using the parameter values that were established for running/walking placental mammals, computing an individual non-Cricetid Rodent's mass from its characteristic length with equation (3) only requires specifying its sturdiness factor and its skeletal muscle similarity. Calculating a Cricetid Rodent's body mass from its characteristic length with equation (3) requires specifying its sturdiness factor, geometric similarity and a larger mitochondrion capability quotient than that used for other Rodentia and non-Musteletid running/walking placental mammals.

MMLE can predict every BMR and body mass datum from (Kolokotrones et al, 2010) for Rodentia that is shown in Fig. 5 and 7 by using equations (2) and (3) simultaneously. There is no unexplained variance. Body mass is computed with equation (3) as just described. Then the non-ruminant Artiodactyl value of the constant G_r established for running/walking placental mammals is used in equation (2) to compute the Rodent's BMR from its shoulder height and sturdiness factor. Some iteration of this process may be required if the head and body length and/or sturdiness factor is not included with the BMR and body mass data for the animal.

Bats (the order Chiroptera). Bats are second only to rodents in the number of species among mammals. Bats comprise about 12% of families, 16% of genera, and 20% of species of recent Mammals. Their masses range over three orders of magnitude from *Craseonycteris thonglongyai* and *Tylonycteris pachypus* with masses as small as 2g to *Pteropus giganteus* with a mass of as much as 1600g. (Nowak, 1999).

(Nowak, 1999) provides data in grams (g) for approximate minimum and maximum body masses. It also provides in millimeters (mm) approximate head and body lengths, forearm lengths and tail lengths when a tail is present. The data are mostly for genera with very little data for species. There is little data on wing span. From the reference (Nowak, 1999) data 350 individual and 176 taxon-averaged body mass, head and body length and forearm length samples

were obtained (Data S3). (Kolokotrones et al, 2010) provides 85 species-averaged BMR and body mass samples. BMR is given in watts and mass is given in grams (g). Lengths were converted to meters (m) for calculations involving equations (1) through (5).

Bats primary means of locomotion is flying by flapping very flexible membranous wings controlled by multi-jointed fingers (Muijres et al, 2011). Unlike birds, bats use their hind limbs as well as their fore limbs to flap their wings (Norberg, 1981). Bats experience daily and seasonal fluctuations in body mass which they accommodate by changes in wing kinematics that vary among individuals (Iriarte-Diaz et al, 2012). To analyze the applicability of MMLE theory to bats, a characteristic length and a fundamental propulsion frequency related to very complicated flapping wing flight needed to be identified. The characteristic length should be related to wing dimensions. (Norberg, 1981) found that forearm length scaled with body mass with about the same exponent as wing span. Given the options available with the (Nowak, 1999) data, it was assumed that forearm length is linearly related to characteristic length. A possible complication that is avoided by this assumption is that full wing dimensions, such as wing span, in a flying bat may vary with flight mode and speed and may be different than those measured from specimens stretched out flat on a horizontal surface (Riskin et al, 2010).

(Norberg & Rayner, 1987) found that geometric similarity applied for most bat wing dimensions with some exceptions. Considering wing span, geometric similarity did not apply for all bats considered together at the 5% level of significance. It did apply to all bat families except the Vesperilionidae. It did apply to primary insectivores, carnivores and nectarivores but not to primary frugivores. More recent work suggests that wing bone lengths are also geometrically similar with respect to body mass in different sized bats (Norberg & Norberg, 2012).Thus geometric similarity, with some exceptions, seems to be the most promising path to identifying a characteristic length and fundamental propulsion frequency related to wing dimensions for bats. For MMLE theory, geometric similarity implies that the slope for the log of body mass regressed on the log of characteristic length is 3.0 and the slope of the log of BMR regressed on the log of body mass is 0.6667.

Table 3 shows the PI and AVG regression analysis results obtained with the (Nowak, 1999) forearm length data and the (Kolokotrones et al, 2010) BMR data. Geometric similarity does not apply to all bats considered together.

The order Chiroptera is divided into two suborders: the Megachiroptera consisting of the single family Peteropodidae and the Microchiroptera consisting of all other bats (Nowak, 1999). From table 3, geometric similarity applies to neither suborder. The mass scaling exponent x for equation (4) is approximately 2.5 for both AVG and PI regressions for Microchiroptera which would indicate y = 0.8. As will be discussed shortly, for bats y = 2/3 is better supported by the data.

Table 3. Results of Bat regression Analyses

Order or Family	Regression Type	Independent Variable	Dependent Variable	Slope	Intercept	R^2	Number Samples
All Bats	PI(0.93)	Length(mm)	Mass(g)	2.6668	-3.3211	0.8507	176
	AVG	Length(mm)	Mass(g)	2.7718	-3.3628	0.9924	NA
Megachiroptera	PI(0.33)	Length(mm)	Mass(g)	2.8628	-3.4933	0.9749	40
	AVG	Length(mm)	Mass(g)	2.7335	-3.2632	0.9978	NA
Microchiroptera	PI(0.93)	Length(mm)	Mass(g)	2.515	-3.1025	0.7522	136
	AVG	Length(mm)	Mass(g)	2.5292	-2.9844	0.9928	NA
Heavy Bats	PI(0.79)	Length(mm)	Mass(g)	2.7595	-3.3252	0.922	86
	AVG	Length(mm)	Mass(g)	2.7233	-3.2329	0.9937	NA
Light Bats	PI(0.0)	Length(mm)	Mass(g)	3.28	-4.4926	0.8781	29
	AVG	Length(mm)	Mass(g)	2.9878	-3.9552	0.9743	NA
All Bats	PI(0.83)	Mass(g)	BMR(watts)	0.8111	-1.9063	0.8784	84
Megachiroptera	PI(0.56)	Mass(g)	BMR(watts)	0.8581	-2.0161	0.9279	21
Microchiroptera	PI(1.07)	Mass(g)	BMR(watts)	0.7459	-1.8247	0.991	63
Heavy Bats	PI(0.89)	Mass(g)	BMR(watts)	0.8225	-1.9166	0.8887	51
Light Bats*	PI(0.0)	Mass(g)	BMR(watts)	0.7015	-1.8048	0.8154	17

The regression expressions are: Log(dependent variable) = slope X log(independent variable) + intercept. PI(n) means the phylogenetic informed regression method using BayesTraits and the number in parentheses is the estimated value of lambda. AVG means the cohort averaging regression method. Length(mm) is forearm length in millimeters. Mass(g) is body mass in grams. NA means Not Applicable. *Data available for only 4 of the 8 families comprising light

The situation in which log body mass for all members of an order scaled with a slope that is less than that expected for geometric similarity was encountered with rodents. In that case it indicated that the order was composed of two subpopulations: one in which geometric similarity applied and another in which a different type of similarity applied. Figure 8 offers such an explanation for bats. In Fig. 8 the bat families have been divided into three groups: 'heavy' bats, 'light' bats and 'intermediate' bats. At the same forearm length members of families composing the heavy bats are mostly more massive than those of the families composing the light bats. Intermediate bats span both the heavy and light mass regimes. The families composing the three groups are given in the caption of Fig. 8.

Table 3 shows that the log body mass slope for light bats is greater than the log body mass slope for heavy bats. For the AVG regression of log mass on log forearm length the slope for light bats is very nearly the 3.0 expected for geometric similarity. The PI regression slope is even greater.

Pteropodidae and Phyllostomidae comprise the heavy bats. The Pteropodidae contain the Old World frugivores and the Phyllostomidae contain the New World frugivores. While both families

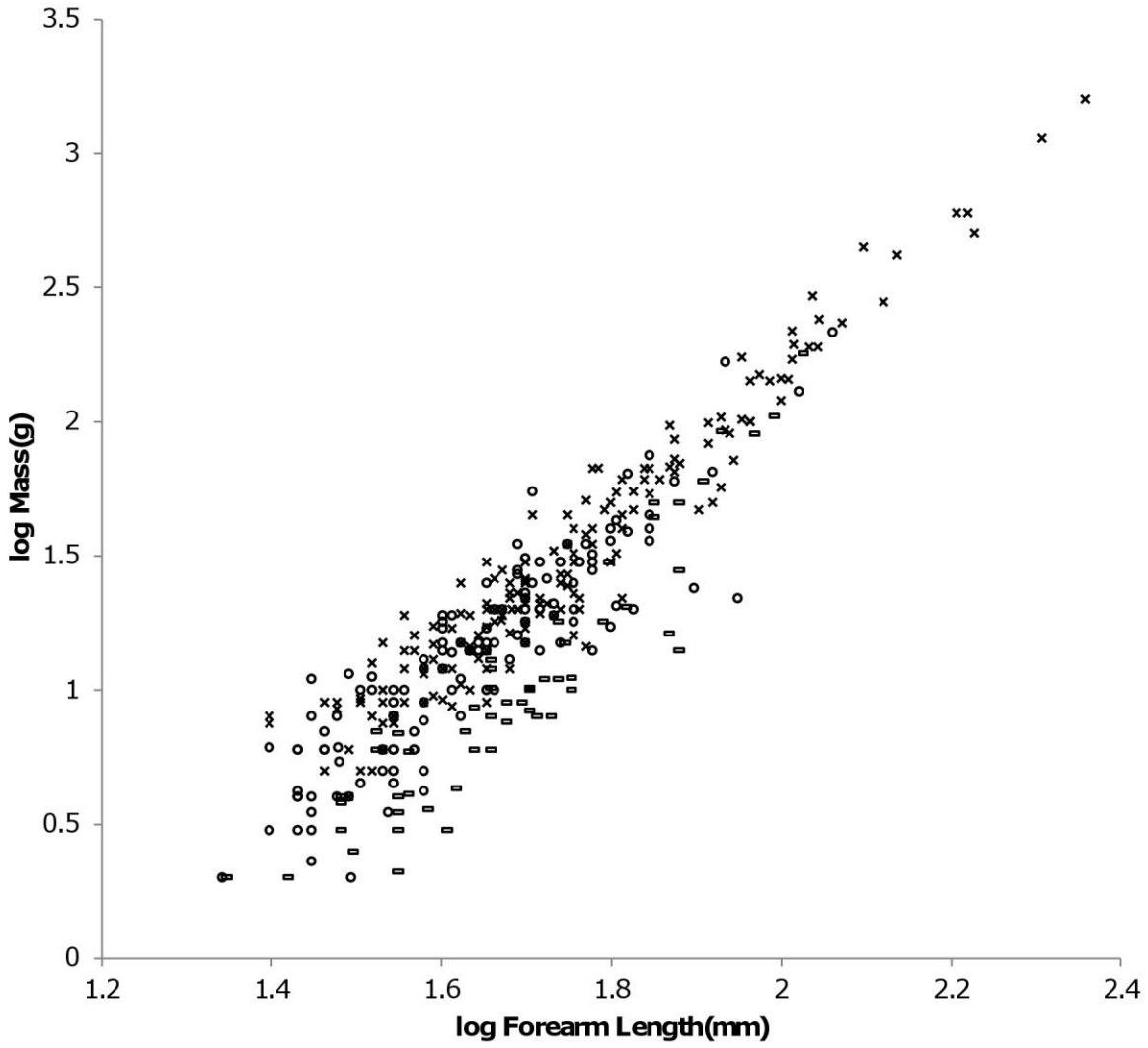

Figure 8. Log body mass as a function of log forearm length for bats. Data are from (Nowak, 1999). At the same forearm length individuals from families composing the 'heavy' bats marked with Xes are mostly more massive than those from the families composing the 'light' bats marked with open rectangles. 'Intermediate' bats marked with open circles span both the heavy and light mass regimes. The families Pteropodidae and Phyllostomidae comprise the heavy bats. The families Emballonuridae, Craseonycteridae, Rhinopomatidae, Rhinolophoidea, Mormoopidae, Noctilionidae, Furipteridae and Hipposideridae comprise the light bats. The families Nycteridae, Megadermatidae, Vespertilionoidae, Thyropteridae, Myzopodidae, Natalidae, Mystacinidae, and Molossidae comprise the intermediate bats.

have species with other diets, the frugivores have wings adapted to commuting long distances from roost to feeding areas (Norberg & Rayner, 1987).The relationships between wing dimensions and body mass should be similar for the frugivore members of the two families.

The fundamental propulsion frequency for bats should be related to the wing flapping frequency. A bat's wing flapping frequency increases slightly with air speed at lower speeds. It becomes almost independent of speed at higher speeds. The speed at which the transition occurs is the preferred speed (Bullen & McKenzie, 2002). The wing flapping frequency at this preferred speed should be proportional to the fundamental propulsion frequency.

Animals that fly by flapping wings operate in a narrow range of Strouhal numbers in cruising flight (Taylor, Nudds & Thomas, 2003). Strouhal number does not change significantly for Pteropodidae (Riskin et al, 2010) . It appears to be an accurate predictor of wingbeat frequency for birds (Nudds, Taylor & Thomas, 2004). Thus Strouhal dynamic similarity is a prime candidate for the type of dynamic similarity that determines the fundamental frequency of propulsion for bats.

As noted in the summary of MMLE theory the fundamental frequency of propulsion would be proportional to the inverse square of the characteristic length if both Strouhal and Reynolds dynamic similarity applied simultaneously. By equation (3) this would result in body mass being proportional to the characteristic length raised to a power greater than 3. This situation is not observed in the Table B-1 regression results except for PI mass regressed on forearm length for light bats. However since the AVG result is so close to geometric similarity this was interpreted as support for geometric similarity with y = 2/3 as was done with Cricetidae Rodentia. It is noted that the characteristic length for viscous drag and that for vortex growth and shedding could be different body dimensions.

For bats Strouhal number =(wingbeat frequency)X(wingbeat amplitude)/(air speed). Wingbeat amplitude is the vertical distance the wing tip travels during a stroke. Under Strouhal dynamic similarity the wingbeat amplitude should be proportional to the MMLE characteristic length. It was assumed that wingbeat amplitude characteristic length is a fraction of forearm length for bats.

Strouhal dynamic similarity is consistent with geometric similarity. Since the fundamental propulsion frequency under geometric similarity is proportional to the inverse of the characteristic length, simultaneous geometric and Strouhal similarity imply that the preferred flight speed is approximately constant.

Assuming geometric similarity and sturdiness boundaries of $(3)^{0.5}$ and$(3)^{-0.5}$ in equations (2) and (3), the scaling fraction linearly relating forearm length to characteristic length for light bats was varied until R_M^2 for BMR was maximized. The corresponding value for the characteristic length scaling fraction is 0.61 meaning that characteristic length is approximately 0.61 of forearm

length. The maximized R_M^2 for BMR is 0.9984. R_M^2 for BMR was used because R_M^2 for body mass was a constant 1.0 over the range of scaling fractions examined from 0.6 to 1.0.

The forearm length is 47.9mm for the mid point of the light bat log forearm lengths. The associated body mass is 11.6g by the AVG regression relationship of table 3. Using these values of forearm length and body mass for geometrically similar light bats, equations (3) was solved for the combined fundamental propulsion frequency and dynamic similarity constants, kc, for each value of the characteristic length scaling fraction. For the value of 0.61 for the scaling fraction, kc = 0.625 m/sec. The running/walking placental mammal derived values for the constants G_m, e and G_o were used in equation (3) and the carnivore derived value for G_r was used in equation (2).

Figure 9 shows the MMLE BMR as a function of body mass boundaries for geometric similarity for light bats evaluated with these estimates together with the (Kolokotrones et al, 2010) BMR and body mass samples for light bats.

A methodology similar to that used for light bats was used to establish the characteristic length scaling fraction and fundamental propulsion frequency constant for heavy bats. By the heavy bat regression relationships of table 3, heavy bats are not geometrically similar. Since heavy bats are not geometrically similar the exponent, r, in the relationship between fundamental propulsion frequency and characteristic length in equations (3) and (5) also had to be established.

The forearm length is 75.9mm for the mid point of the heavy bat log forearm lengths. The corresponding body mass is 77.1g by the AVG regression relationship and 73g for the PI relationship. The value of x in equation (4) is 2.72 for the AVG regression relationship and 2.76 for the PI relationship of table 3. Both values of x are consistent with y = 2/3. These values were used in equations (3) and (5) to solve for the characteristic length scaling fraction, the exponent r and the combined fundamental propulsion frequency and dynamic similarity constants, kc. This was done by varying r for each trial value of the characteristic length scaling fraction until a pair of values for the characteristic scaling fraction and r was found that maximized R_M^2 for BMR. For the AVG relationship the value for the characteristic scaling fraction is 0.92, the value for the exponent r is 0.68 and the value for the combined fundamental propulsion frequency and dynamic similarity constants is kc = 3.22 $m^{0.68}$/sec. The corresponding value of R_M^2 for BMR is 0.9828. For the PI relationship the value for the characteristic scaling fraction is 0.86, the value for the exponent r is 0.73 and the value for the combined fundamental propulsion frequency and dynamic similarity constants is kc = 2.59 $m^{0.73}$/sec. The corresponding value of R_M^2 for BMR is 0.9918. As with light bats, R_M^2 for BMR was used because R_M^2 for body mass was very nearly 1.0 over the range of parameters examined. In terms of R_M^2 the PI and AVG results are nearly indistinguishable.

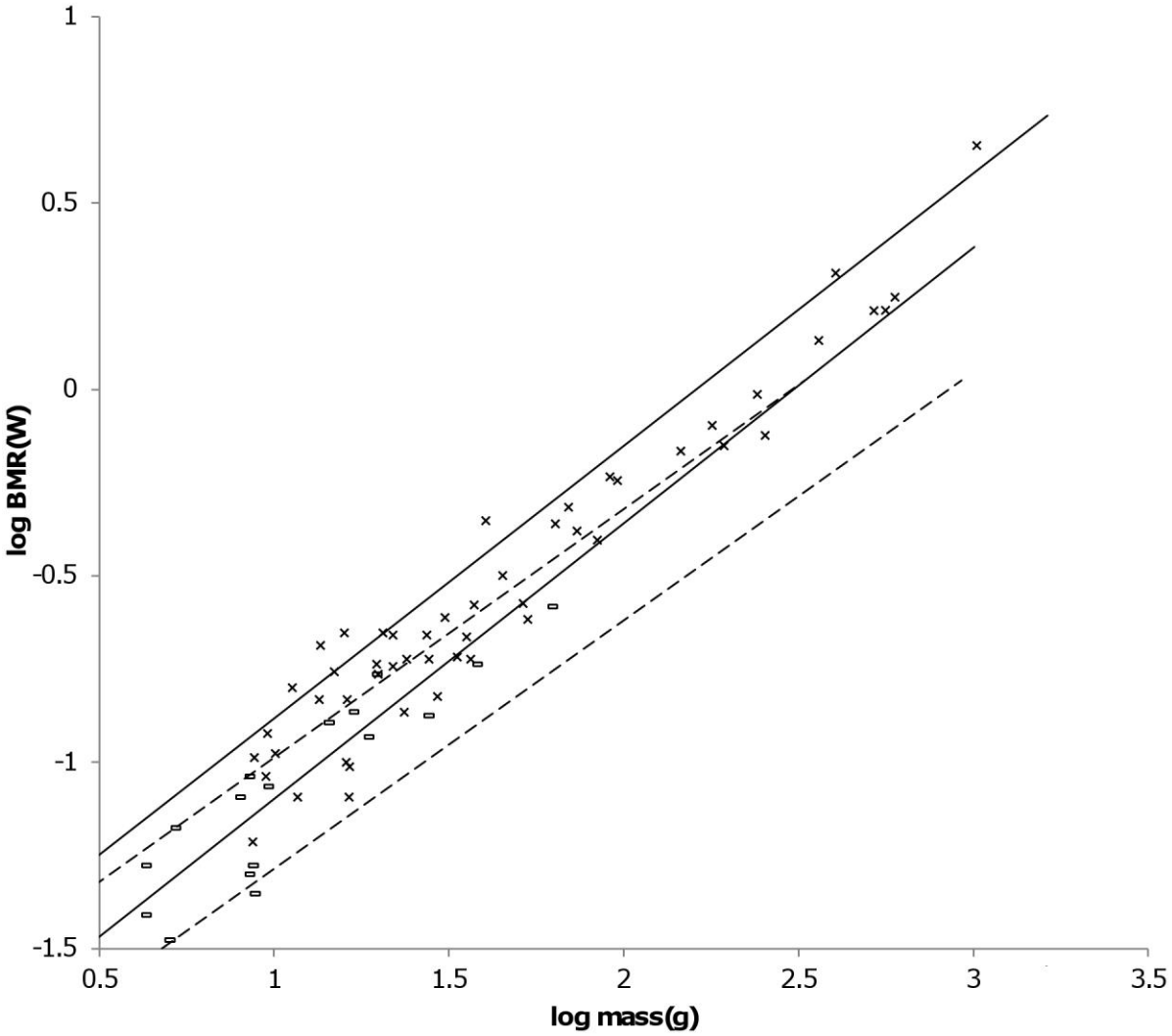

Figure 9. Log BMR as a function of log body mass for heavy and light bats. Data are from (Kolokotrones et al, 2010). The solid and dashed lines are the MMLE sturdiness factor boundaries. The upper boundaries were generated with a sturdiness factor $s = (3)^{0.5}$. The lower boundaries were generated with $s = (3)^{-0.5}$. The steeper sloping solid boundary lines are for heavy bat Strouhal dynamic similarity. The shallower sloping dashed boundary lines are for light bat geometric similarity. $R_M^2 = 0.9828$ for heavy bats with respect to the Strouhal boundaries. $R_M^2 = 0.9984$ for light bats with respect to the geometric boundaries. Heavy bat species-averaged data are marked with Xes. Light bats species-averaged data are marked with open rectangles. Data was available for only four of the eight families comprising the light bats.

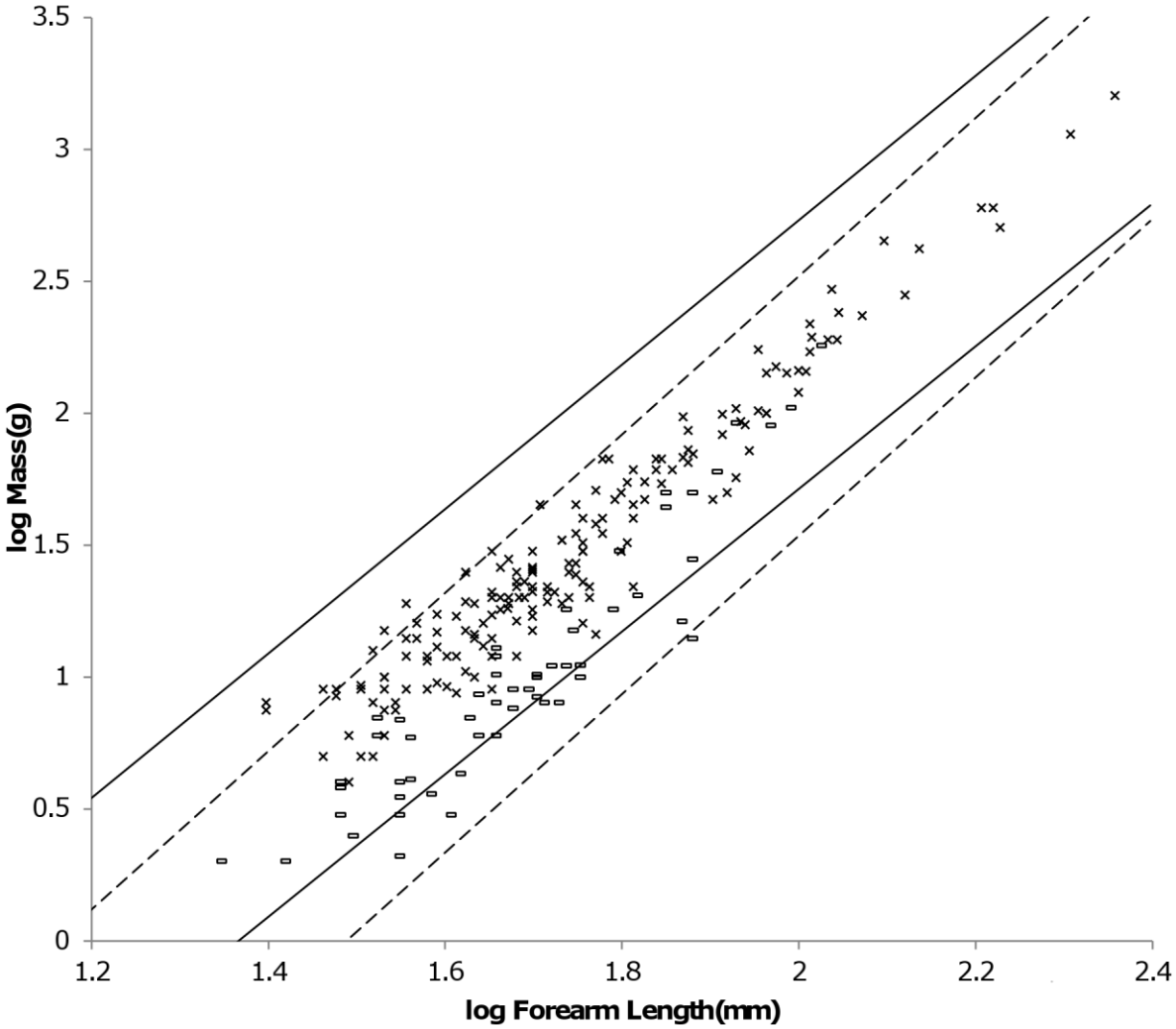

Figure 10. Log body mass as a function of log forearm length for heavy and light bats. Data are from (Nowak, 1999). The solid and dashed lines are the MMLE sturdiness factor boundaries. The upper boundaries were generated with a sturdiness factor $s = (3)^{0.5}$. The lower boundaries were generated with $s = (3)^{-0.5}$. The shallower sloping solid boundary lines are for heavy bat Strouhal dynamic similarity. The steeper sloping dashed boundary lines are for light bat geometric similarity. The data are from (Nowak, 1999). $R_M^2 = 0.9982$ for heavy bats with respect to the Strouhal boundaries. $R_M^2 = 1.0$ for light bats with respect to the geometric boundaries. Individual heavy bats are marked with Xes. Individual light bats are marked with open rectangles.

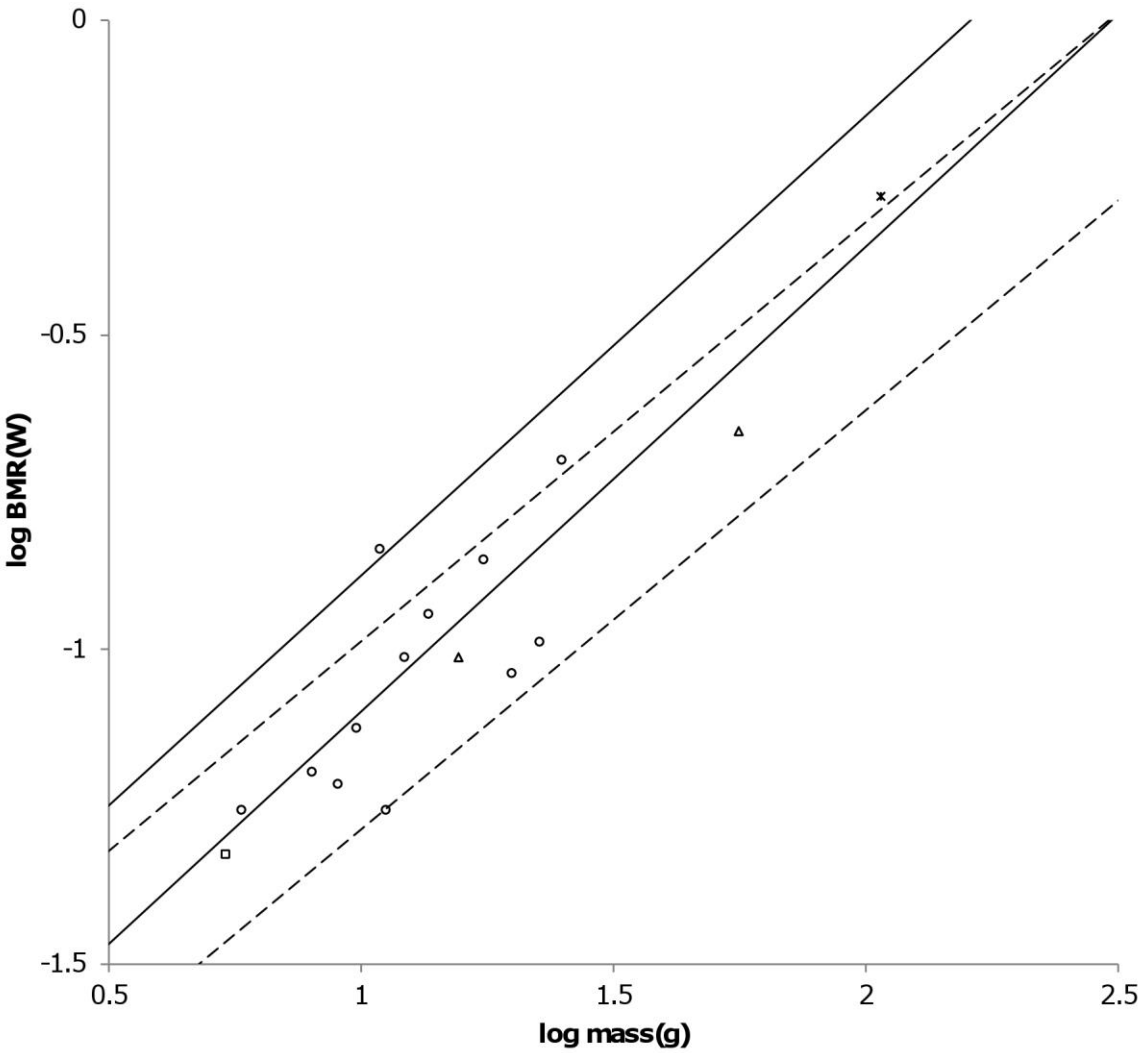

Figure 11. Log BMR as a function of log body mass for intermediate bats. Data are from (Kolokotrones et al, 2010). The solid and dashed lines are the MMLE sturdiness factor boundaries. The upper boundaries were generated with a sturdiness factor $s = (3)^{0.5}$. The lower boundaries were generated with $s = (3)^{-0.5}$. The steeper sloping solid boundary lines are for heavy bat Strouhal dynamic similarity. The shallower sloping dashed boundary lines are for light bat geometric similarity. Data was available for only four of the eight families comprising the intermediate bats. $R_M^2 = 0.9678$ for intermediate bats with respect to the Strouhal boundaries. $R_M^2 = 0.9893$ for intermediate bats with respect to the geometric boundaries. $R_M^2 = 0.9998$ for intermediate bats with respect to both sets of boundaries. The data are species-averaged. Megadermatidae are marked with crossed Xes. Molossidae are marked with open triangles. Vesperstilionidae are marked with open circles. Natalidae are marked with open squares.

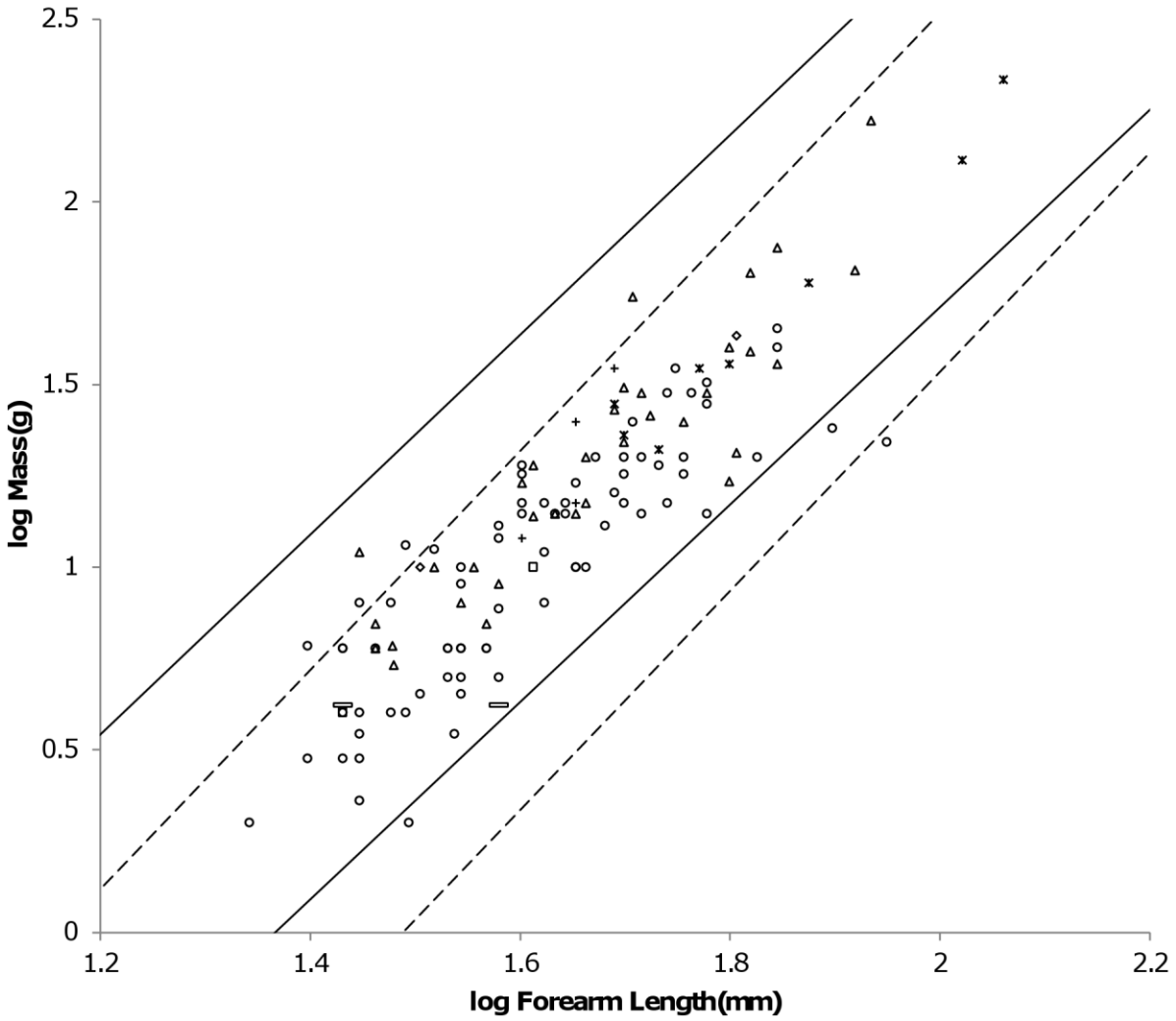

Figure 12. Log body mass as a function of log forearm length for intermediate bats. Data are for individuals from (Nowak, 1999). The solid and dashed lines are the MMLE sturdiness factor boundaries. The upper boundaries were generated with a sturdiness factor $s = (3)^{0.5}$. The lower boundaries were generated with $s = (3)^{-0.5}$. The shallower sloping solid boundary lines are for heavy bat Strouhal dynamic similarity. The steeper sloping dashed boundary lines are for geometric similarity. $R_M^2 = 0.998$ for intermediate bats with respect to the Strouhal boundaries. $R_M^2 = 0.9981$ for intermediate bats with respect to the geometric boundaries. $R_M^2 = 0.9999$ for intermediate bats with respect to both sets of boundaries.

Figure 9 also shows the MMLE log BMR as a function of log body mass MMLE sturdiness factor boundaries for heavy bats evaluated with these estimates together with the (Kolokotrones et al, 2010) species averaged BMR and body mass samples for heavy bats.

Figure 10 shows the MMLE log body mass as a function of log forearm length MMLE sturdiness factor boundaries for both heavy bats and geometrically similar light bats. The (Nowak, 1999) heavy and light bat mass and forearm length data are also shown.

Because the exponent r in equation (3) is less than unity for heavy bats, the fundamental propulsion frequency should scale with bat dimensions differently than what would be expected for geometric similarity. Also the Strouhal number or preferred flight speed, or both, should scale with body dimensions. For Megachiroptera, the inverse of wingbeat frequency scales with body mass significantly more shallowly than expected with geometric similarity. Both Strouhal number and preferred flight speed scale very slightly with body mass but this is not considered to be significant (Riskin et al, 2010).

From table 3 the AVG regression relationship between body mass and forearm length are nearly identical for heavy bats and the Megachiroptera suborder of bats. Body mass approximately scales as forearm length raised to the 2.72 power. The coefficient of determination, R^2, is almost 1.0 which allows the mass-length relationship to be accurately inverted so that forearm length scales as body mass raised to the 0.37 power. Since the heavy bat fundamental propulsion frequency, f, scales as forearm length raised to the -0.68 power, f scales as body mass raised to the -0.25 power. (Norberg & Norberg, 2012) found f scaled as mass raised to the -0.276 power, $R^2 = 0.932$, for Megachiroptera.

Figure 11 shows the MMLE log BMR as a function of log body mass MMLE sturdiness factor boundaries for both heavy bats and light bats. The (Kolokotrones et al, 2010) species averaged BMR and body mass samples for intermediate bats are also shown. The data spreads over both MMLE bands as if within the same family there are species that conform to geometric similarity and other species that conform to heavy bat similarity.

Figure 12 shows the MMLE log body mass as a function of log forearm length MMLE sturdiness factor boundaries for both heavy and light bats. The (Nowak, 1999) body mass and forearm length samples for intermediate bats are also shown. Intermediate bat body mass is explained almost equally well by either the geometrically similar light bat MMLE band or the heavy bat MMLE band. $R_M^2 = 0.9981$ for the light bat MMLE band. $R_M^2 = 0.9980$ for the heavy bat MMLE band. $R_M^2 = 0.9999$ for the two bands together.

The light and heavy bat data in Fig. 10 does not fully occupy their respective MMLE sturdiness factor bands. This raises the possibility that a sturdiness factor range narrower than $(3)^{-0.5}$ to $(3)^{0.5}$ may apply to heavy or light bats. The intermediate bat data in Fig. 12 more completely occupies both bands indicating that the full sturdiness factor range is applicable. The situation may be more complicated. Each of the heavy, light and intermediate bat groups contains species with

different food habits. Bat wing morphology is associated with flight behavior related to food habits. Even among the insectivores that dominate the light and intermediate groups there are different styles of catching insects that are associated with differing wing morphologies (Norberg & Rayner, 1987; Norberg & Norberg, 2012). Dynamic similarity may apply at a phylogenetic level below the family.

The light-intermediate-heavy representation of bats is better supported by the data than either the all bats representation or the Megachiroptera-Microchiroptera representation in terms of R_M^2 and coverage, R. For mass and forearm length both R_M^2 and R are very nearly 1.0 for all three representations. For BMR and body mass $R_M^2 = 0.9882$ and $R = 0.73$ for the all bats representation when computed using the AVG mass and forearm length regression relationship in table 3 but they reduce to $R_M^2 = 0.9418$ and $R = 0.39$ when using the PI relationship. For the light-intermediate-heavy representation the combined $R_M^2 = 0.99$ and the combined $R = 0.7$ using both the PI and the AVG relationships. For the Megachiroptera-Microchiroptera representation the combined $R_M^2 = 0.98$ and the combined $R = 0.4$ using either relationship. The poorer performance of the Megachiroptera-Microchiroptera representation is due to low coverage of Microchiroptera data computed with $y = 0.8$ which is consistent with both the PI and AVG relationships in table 3: R is only 0.24 for the Microchiroptera data.

MMLE can exactly predict every individual body mass, head and body length datum from (Nowak, 1999) for bats that is shown in Fig. 8, 10 and 12. There is no unexplained variance. A separate characteristic length scaling fraction is needed for light bats and for heavy bats to translate the available forearm length data to characteristic lengths. Then using the parameter values that were established for running/walking placental mammals, computing an individual light bat's body mass from its forearm length with equation (3) requires specifying its sturdiness factor, geometric muscle similarity and the light bat combined fundamental propulsion frequency and dynamic similarity constants, kc. Computing a heavy bat's body mass from its forearm length with equation (3) requires specifying its sturdiness factor, the heavy bat fundamental propulsion frequency exponent, r, and the heavy bat combined fundamental propulsion frequency and dynamic similarity constants, kc. Computing an intermediate bat's body mass from its forearm length may require evaluating the animal as a light bat and as a heavy bat and then deciding which classification better agrees with the datum.

MMLE can also predict every BMR and body mass datum from (Kolokotrones et al, 2010) for bats that is shown in Fig. 9 and 11 by using equations (2) and (3) simultaneously. There is no unexplained variance. Body mass is computed with equation (3) as just described. Then the Carnivore value of the constant G_r established for running/walking placental mammals is used in equation (2) to compute the bat's BMR from its forearm length and sturdiness factor. Some iteration of this process may be required if the head and body length and/or sturdiness factor is not included with the BMR and body mass data for the animal.

Discussion. MMLE can exactly predict body mass as a function of characteristic length for at least the placental mammal orders Rodentia, Chiroptera, Artiodactyla, Carnivora, Perissodactyla and Proboscidae. There is no unexplained variance. Furthermore MMLE can exactly predict BMR as a function of body mass for at least the orders Rodentia, Chiroptera, Artiodactyla and Carnivora without any unexplained variance.

The ability of MMLE to exactly predict every datum obtained from the appropriate data set does not necessarily mean that there is no unexplained variance with MMLE theory. Equations (2) and (3) apply simultaneously to a particular individual animal which has particular values for body mass, BMR, and characteristic length. The author of the present paper is unaware of a data set that reports all three of these values for individual animals. Instead there is the data set from (Nowak, 1999) reporting individual body mass and characteristic length and another data set from (Kolokotrones et al, 2010) that reports species-averaged BMR and body mass. It is unlikely that the same particular animal is included in both data sets. There is likely to be unexplained variance with a data set that simultaneously reports the three values of mass, BMR and length for individual animals. The unexplained variance would be detected by the need to use one value of the sturdiness factor in equation (3) to accurately predict mass and a different value in equation (2) to accurately predict BMR for the same animal.

That there would be unexplained variance with a data set that reports the three values of mass, BMR and length for individual animals is suspected because MMLE theory as currently expressed does not account for body temperature effects on the mitochondrion capability quotient. Body temperature has a significant effect on BMR (Clarke, Rothery & Isaac, 2010; Kolokotrones et al, 2010). The extent to which the inclusion of temperature effects on the mitochondrion capability quotient would improve MMLE's accuracy awaits a complete data set reporting body temperature as well as mass, BMR and length for individual animals. In the meantime, the body temperature data in (Kolokotrones et al, 2010) could be used to examine the extent to which inclusion of temperature in equation (3) would narrow the sturdiness factor range needed to bound the (Kolokotrones et al, 2010) BMR and mass data and the (Nowak, 1999) mass and length data.

Ten parameters were theoretically derived to predict BMR and body mass with MMLE. The skeletal muscle mass constant, G_m and the non-skeletal muscle mass constant, G_o should have the same values for all placental mammals. The non-skeletal muscle mass exponent, y with its associated dimensionality factor m, used in equation (3) to predict body mass may have at least two values although the results predicted with the two values are nearly indistinguishable for the group of animals to which they may apply: runners/walkers . The type of similarity applicable to an animal's skeletal muscles determines the values for the dynamic similarity constant, k, the fundamental propulsion frequency constant, c, and the fundamental propulsion frequency exponent, r, used in equation (3). The mitochondrion capability quotient, e, used in equation (3) should have the same approximate value for all animals with the same body temperature in the same phylogenetic group. Whether an animal is a ruminant Artiodactyl or not determines which

value of the resting metabolic rate constant, G_r, to use in equation (2) to predict BMR. Finally, the characteristic length, l, and the sturdiness factor, s, for an individual animal is used in equations (2) and (3) to predict that animal's BMR and body mass. If the characteristic length is not available then an eleventh parameter, a scaling fraction, can be used to translate the available length datum into the characteristic length.

The results of regression analyses were used to estimate numerical values for the parameters. Phylogenetically informed (PI) regression analysis was performed on taxon-averaged data using BayesTraits. AVG regression analysis was performed on individual body mass, characteristic length data. AVG regression is unique to MMLE theory. Parameter numerical values estimated from results obtained with the two regression techniques did differ. Commenting on which regression technique is superior was not a purpose of the present paper. In terms of the two MMLE measures of effectiveness, R_M^2 and R, body masses predicted by equation (3) and BMR predicted by equation (2) are nearly indistinguishable when using parameters estimated from the results of either technique.

The results of the regression analyses were also used to partition populations into animals that conform to geometric similarity and animals that do not. Geometric similarity implies that body mass scales as the cube of characteristic length and BMR scales as body mass raised to the 2/3 power. The body mass of animals that do not conform to geometric similarity scale with characteristic length raised to a power less than three and BMR scales with body mass raised to a power greater than 2/3. Thus the BMR of a mixture of species can appear to scale with body mass raised to a power greater than 2/3 as observed in 1960 by Hemmingsen as cited in (Hulbert & Else, 2004).

As noted in the summary of MMLE theory, ten or eleven parameters is not such a large number of parameters to predict the absolute values of an individual placental mammal's BMR and body mass. Except for the characteristic length scaling fraction, the parameters emerged from the theoretical derivation of MMLE from the principles of physics and physiology that were being considered. The reconciliation of Cricetidae with the rest of Rodentia, the reconciliation of Mustelidae with the rest of Carnivora or the division of bats into three new groups could appear to be forcing MMLE to fit the data. However these instances are legitimate uses of the degrees of freedom available with MMLE to explain differences that were observed in the data.

The values for the constants G_m, G_o and G_r were derived from running/walking placental mammal data. Since the values obtained in the present paper differ from the values obtained with the data that was available over a quarter of a century ago, it would not be surprising if the values should be refined again in the future.

MMLE represents the vertebrate body as being composed of two types of tissues: volume active tissues in which mitochondria are approximately uniformly distributed; and surface active tissues in which the mitochondria are concentrated in surfaces that surround material with few

mitochondria. The volume active tissues are associated with the skeletal musculature whose morphology is governed by dynamic similarity. The surface active tissues are associated with liver, heart, kidneys, and brain which is better represented as geometrically similar for Rodentia and Bats. For the mass of running/walking Artiodactyla and Carnivora predicted by equation (3) a geometrically similar representation in which surface area scales as volume raised to the 2/3 power is nearly indistinguishable from a topology in which surface area scales as volume raised to the 4/5 power.

Using equation (3) the ratio of volume active tissue mass to total body mass for geometrically similar running/walking placental mammals is calculated to vary form 81% for sturdy animals to 93% for gracile animals. For Strouhal-Froude dynamically similar animals the ratio varies from 87% for small sturdy animals to 91% for small gracile animals; and for large animals it varies from 61% for sturdy animals to 74% for gracile animals. The ratio of muscle to total body mass appears to vary between 21% and 61% for mammals (Muchlinski, Snodgrass & Terranova, 2012). The MMLE volume active tissues appear to be about twice as massive as the skeletal musculature. This leads to the possibility that inclusion of a third type of tissue in the MMLE representation of the vertebrate body may be warranted. The third tissue type would include everything that is not skeletal muscle, liver, heart, kidneys, and brain. It would have few mitochondria so that it would contribute little to BMR.

Three types of dynamic similarity were encountered for the skeletal musculature of the placental mammals examined in the present paper: Froude similarity, Strouhal similarity and simultaneous Froude and Strouhal similarity. Geometric similarity is compatible with either Froude or Strouhal similarity. It is not compatible with simultaneous Froude and Strouhal similarity. The type of dynamic similarity that governs the morphology of an animal's skeletal musculature seems to correlate with a phylogenetic level that may be as low as the species.

Compared with the original paper (Frasier, 1984), the present paper makes important modifications to MMLE theory. The fundamental propulsion frequency is generalized to $f = c/l^r$ where c is the fundamental propulsion frequency constant, l is the characteristic length and r is the fundamental propulsion frequency exponent. This generalization allows the different types of dynamic similarity to be excitedly addressed by equation (3). The mass of the non-skeletal musculature is also generalized to allow non-geometrically similar topologies to be explicitly addressed by equation (3). Ordinary Least Squares regression analyses are replaced by PI analyses in the present paper. The present paper estimates new numerical values for the parameters occurring in equations (2) and (3) by analysis of data that was unavailable when the original paper was written. The present paper furthermore extends the demonstration of MMLE theory's ability to exactly predict body mass and BMR for individual animals from about 9% of placental mammals to about 72% by adding Rodentia and bats to running/walking Artiodactyla, Carnivora, Perissodactyla and Proboscidae.

Carnivora with body masses less than about 2000g were not included in the body mass as a function of characteristic length analysis of running/walking placental mammals. They were not included because their shoulder heights are not given in (Nowak, 1999). However head and body lengths are given. The methodology of using a scaling fraction to translate heady and body length to characteristic length as was done for Rodentia may also work for small Carnivora.

MMLE's ability to predict BMR and body mass for the mammal orders that were not included in the present paper should be examined. A complication is that from an examination of (Kolokotrones et al, 2010) it appears that BMR data are scarce except for the orders Primates, Soricomorpha, Dasyuromorpha and Diprotodontia.

MMLE should apply to all vertebrates. The original paper tried to address birds but that analysis now appears to be simplistic. The analysis should be performed again with recent data and the expanded version of MMLE presented in the present paper.

The examination of body mass and BMR from the skeletal length perspective rather than from the body mass perspective lead to the concept of the sturdiness factor in MMLE theory. The sturdiness factor adds additional information about the composition of an animal's body that is missing from relationships of the form aW^b. Consideration of body composition can reduce unexplained variance even for relationships that express BMR as a function of body mass (Raichlen et al, 2010; Müller et al, 2011). MMLE explains all the variance for an animal's BMR and body mass. Compared to the variance explained by the PI regression relationships of the form $BMR = aW^b$ in tables 1, 2 and 3, MMLE explains an additional 2.5% to 18.5% of the variance. The sturdiness factor is a major contributor to this additional explained variance.

The (Raichlen, Pontzer & Shapiro, 2013) finding that hip joint to limb center of mass length is a better length for establishing the pendulum frequency for Froude-Strouhal similar animals may affect the concept of the sturdiness factor. Sturdier animals have stouter limbs which should cause the limb's center of mass to be further from the hip joint and thereby increase the characteristic length. For this reason it is possible that the sturdiness factor may be, in part, a scaling factor for converting characteristic length surrogates such as shoulder height into hip joint to limb center of mass lengths.

While the mitochondrion capability quotient used in equation (3) should have approximately the same value for all animals with the same body temperature in the same phylogenetic group, genetic variation could cause it to vary among individuals or populations in the same species. Variation of the mitochondrion capability coefficient together with variation of the sturdiness factor would cause mass-independent variation in the BMR of animals like that recently addressed by White and Kearney (White & Kearney, 2013).

MMLE was derived for fit animals surviving in the wild. Captivity, domestication, inactivity and sickness could cause an animal's body mass or BMR to be different from that predicted by

MMLE. In particular, muscle or mitochondrion atrophy due to decreased activity with respect to that experienced in the wild would likely cause a difference.

Conclusion. The purpose of this paper was to use modern resources to revisit MMLE theory and test its ability to predict the absolute values of BMR and body mass for individual animals. With some modifications to the theory as originally formulated (Frasier, 1984) MMLE can exactly predict an individual animal's BMR given its body mass and its body mass given its characteristic length for the recent data sets that were examined (Nowak, 1999; Kolokotrones et al, 2010) and for the mammal orders examined. The examined mammal orders include over two thirds of recent mammal species.

Determining if MMLE can simultaneously exactly predict an individual animal's BMR and body mass given its characteristic length awaits a data set that simultaneously reports all three values for individual animals.

Supplemental Information.

Data S1.

Running-walking placental mammals masses and shoulder heights.

Data S2.

Rodentia masses and lengths.

Data S3.

Chiroptera (Bats) masses and lengths.

Acknowledgements. I thank Olaf Bininda-Emonds for identifying the most recent mammal phylogenetic tress and for outlining how to graft Carnivora (Nyakatura & Bininda-Emonds, 2013) to the rest of Mammalia (Fritz, Bininda-Emonds & Purvis, 2009). I also thank the anonymous reviewers for constructive comments.

References.

Agutter PS, Tuszynski JA. 2011. Analytic theories of allometric scaling. *The journal of experimental biology* 214: 1055-62.

Alexander RM, Jayes AS, Malioy GM, Wathuta EM. 1979. Allometry of the limb bones of mammals from shrews Sorex. to elephant Loxodonta.. *Journal of zoology : proceedings of the Zoological Society of London* 189: 305-314.

Alexander RM. 2005. Models and the scaling of energy costs for locomotion. *The journal of experimental biology* 208: 1645-52.

Banavar JR, Moses ME, Brown JH, Damuth J, Rinaldo A, Sibly RM, Maritan A. 2010. A general basis for quarter-power scaling in animals. *Proceedings of the National Academy of Sciences of the United States of America* 107: 15816-20.

Biewener AA. 2005. Biomechanical consequences of scaling. *The journal of experimental biology* 208: 1665-76.

Bullen RD, McKenzie NL. 2002. Scaling bat wingbeat frequency and amplitude. *The journal of experimental biology* 205: 2615-26.

Campione NE, Evans DC. 2013. A universal scaling relationship between body mass and proximal limb bone dimensions in quadrupedal terrestrial tetrapods. *BMC biology* 10:60.

Capellini I, Venditti C, Barton RA. 2010. Phylogeny and metabolic scaling in mammals. *Ecology* 91: 2783-93.

Christiansen P. 1999. Scaling of the limb long bones to body mass in terrestrial mammals. *Journal of Morphology* 239: 167-90.

Clarke A, Rothery P, Isaac NJ 2010. Scaling of basal metabolic rate with body mass and temperature in mammals. *The Journal of animal ecology* 79: 610-9.

da Fonseca RR, Johnson WE, O'Brien SJ, Ramos MJ, Antunes A. 2010. The adaptive evolution of the mammalian mitochondrial genome. *BMC Genomics* 9: 119.

Economos AC. 1982. On the origin of biological similarity. *Journal of theoretical biology* 94: 25-60.

Edwards AL. 1984. *An introduction to linear regression and correlation*. New York: W. H. Freeman. 32 .

Else PL, Hulbert AJ. 1981. Comparison of the “mammal machine” and the “reptile machine”: energy production. *The American journal of physiology* 240: R3-R9.

1505 Else PL, Hulbert AJ. 1985. An allometric comparison of the mitochondria of mammalian and
1506 reptilian tissues: the implications for the evolution of endothermy. *Journal of comparative*
1507 *physiology. B, Biochemical, systemic, and environmental physiology* 156: 3-11.

1508 Frasier CC. 1984. An explanation of the relationships between mass, metabolic rate and
1509 characteristic length for birds and mammals. *Journal of theoretical biology* 109: 331-371.

1510 Freckleton RP, Harvey PH, Pagel M. 2002. Phylogenetic analysis and comparative data: a test
1511 and review of evidence. *The American naturalist* 160: 712-26.

1512 Fritz SA, Bininda-Emonds OR, Purvis A. 2009. Geographical variation in predictors of
1513 mammalian extinction risk: big is bad, but only in the tropics. *Ecology letters* 2009 12: 538-49.

1514 Garcia GJ, da Silva JK. 2004. On the scaling of mammalian long bones. *The journal of*
1515 *experimental biology* 207: 1577-84.

1516 Glazier DS. 2010. A unifying explanation for diverse metabolic scaling in animals and plants.
1517 *Biological reviews of the Cambridge Philosophical Society* 85: 111-38.

1518 Guderley H, Turner N, Else PL, Hulbert AJ. 2005. Why are some mitochondria more powerful
1519 than others: insights from comparisons of muscle mitochondria from three terrestrial vertebrates.
1520 *Comparative biochemistry and physiology. Part B, Biochemistry & molecular biology* 142: 172-
1521 80.

1522 Hudson LN, Isaac NJ, Reuman DC. 2013. The relationship between body mass and field
1523 metabolic rate among individual birds and mammals. *The journal of animal ecology* 82: 1009-
1524 20.

1525 Hulbert AJ, Else PL 1999. Membranes as possible pacemakers of metabolism. *Journal of*
1526 *theoretical biology* 199: 257-74.

1527 Hulbert AJ, Else PL. 2004. Basal metabolic rate: history, composition, regulation, and
1528 usefulness. *Physiological and biochemical zoology* 77: 869-76.

1529 Iriarte-Diaz J, Riskin DK, Breuer KS, Swartz SM. 2012. Kinematic plasticity during flight in
1530 fruit bats: individual variability in response to loading. *PLoS One.* 7(5): e36665.

1531 Isaac NJ, Carbone C. 2010. Why are metabolic scaling exponents so controversial? Quantifying
1532 variance and testing hypotheses. *Ecology letters* 13: 728-35.

1533 Jastroch M, Divakaruni AS, Mookerjee S, Treberg JR, Brand MD. 2010. Mitochondrial proton
1534 and electron leaks. *Essays in biochemistry* 47: 53-67.

1535 Kleiber M. 1932. Body size and metabolism. *Hilgardia* 6: 315-353.

Kleiber M. 1961. The fire of life: *An introduction to animal energetics*. New York: John Wiley & Sons.

Kolokotrones T, Savage V, Deeds E.J, Fontana, W. 2010. Curvature in metabolic scaling. *Nature* 464: 753-756.

Kozlowski J, Konarzewski M, Gawelczyk AT. 2003. Cell size as a link between noncoding DNA and metabolic rate scaling. *Proceedings of the National Academy of Sciences of the United States of America* 100: 14080-5.

Maino JL, Kearney MR, Nisbet RM, Kooijman SA. 2014. Reconciling theories for metabolic scaling. The Journal of animal ecology 83: 20-29.

McMahon TA. 1973. Size and shape in biology. *Science* 179: 1201-1204.

McMahon TA. 1975. Allometry and biomechanics: limb bones in adult ungulates. *The American naturalist* 109: 547-563.

McNab BK. 1988. Complications inherent in scaling the basal rate of metabolism in mammals. *The Quarterly review of biology* 63: 25-54.

McNab, BK. 1997. On the utility of uniformity in the definition of basal rate of metabolism. *Physiological zoology* 70: 718–720

McNab BK. 2008. An analysis of the factors that influence the level and scaling of mammalian BMR. *Comparative biochemistry and physiology. Part A, Molecular & integrative physiology* 151: 5-28.

Muchlinski MN, Snodgrass JJ, Terranova CJ. 2012. Muscle mass scaling in primates: an energetic and ecological perspective. *American journal of primatology* 74: 395-407.

Muijres FT, Johansson LC, Winter Y, Hedenström A. 2011. Comparative aerodynamic performance of flapping flight in two bat species using time-resolved wake visualization. *Journal of the Royal Society, Interface / the Royal Society* 8: 1418-28.

Müller MJ, Langemann D, Gehrke I, Later W, Heller M, Glüer CC, Heymsfield SB, Bosy-Westphal A. 2011. Effect of constitution on mass of individual organs and their association with metabolic rate in humans--a detailed view on allometric scaling. *PLoS One*. 6(7): e22732.

Müller MJ, Wang Z, Heymsfield SB, Schautz B, Bosy-Westphal A. 2013. Advances in the understanding of specific metabolic rates of major organs and tissues in humans. *Current opinion in clinical nutrition metabolic care.* 16: 501-8.

Norberg UM. 1981. Allometry of Bat Wings and Legs and Comparison with Bird Wings. *Philosophical transactions of the Royal Society of London. Series B, Biological sciences* 292: 359-398.

Norberg, UM, Rayner, JMV. 1987. Ecological morphology and flight in bats Mammalia; Chiroptera.: wing adaptations, flight performance, foraging strategy and echolocation. *Philosophical transactions of the Royal Society of London. Series B, Biological sciences* 316: 335–427.

Norberg UM, Norberg RA. 2012. Scaling of wingbeat frequency with body mass in bats and limits to maximum bat size. *The journal of experimental biology* 215: 711-22.

Nowak RM. 1999. *Walker's mammals of the world*. Baltimore: John Hopkins.

Nudds RL, Taylor GK, Thomas AL. 2004. Tuning of Strouhal number for high propulsive efficiency accurately predicts how wingbeat frequency and stroke amplitude relate and scale with size and flight speed in birds. *Proceedings. Biological sciences / The Royal Society* 271: 2071-6.

Nyakatura K, Bininda-Emonds OR. 2013. Updating the evolutionary history of Carnivora Mammalia.: a new species-level supertree complete with divergence time estimates. *BMC Biology* 10: 12.

Pagel M. 1999. Inferring the historical patterns of biological evolution. Nature. 401: 877-84.

Pagel M, Meade A, Barker D. 2004. Bayesian estimation of ancestral character states on phylogenies. *Systematic Biolology* 2004 53: 673-84.

Raichlen DA, Gordon AD, Muchlinski MN, Snodgrass JJ. 2010. Causes and significance of variation in mammalian basal metabolism. *Journal of comparative physiology. B, Biochemical, systemic, and environmental physiology* 180: 301-11.

Raichlen DA, Pontzer H, Shapiro LJ. 2013. A new look at the dynamic similarity hypothesis: the importance of the swing phase. *Biology open* 19: 1032-6

Riskin DK, Iriarte-Díaz J, Middleton KM, Breuer KS, Swartz SM. 2010. The effect of body size on the wing movements of pteropodid bats, with insights into thrust and lift production. J *The journal of experimental biology* 213: 4110-22.

Roberts MF, Lightfoot EN, Porter WP. 2010. A new model for the body size-metabolism relationship. *Physiological and biochemical zoology* 83: 395-405.

Roberts MF, Lightfoot EN, Porter WP. 2011. Basal metabolic rate of endotherms can be modeled using heat-transfer principles and physiological concepts: reply to "can the basal metabolic rate of endotherms be explained by biophysical modeling?". *Physiological and biochemical zoology* 84: 111-4.

1599 Savage VM, Gillooly JF, Woodruff WH, West GB, Allen AP, et al. 2004. The predominance of
1600 quarter-power scaling in biology. *Functional Ecology* 18: 257-282.

1601 Seebacher F, Brand MD, Else PL, Guderley H, Hulbert AJ, Moyes CD. 2010. Plasticity of
1602 oxidative metabolism in variable climates: molecular mechanisms. *Physiological and*
1603 *biochemical zoology : PBZ* 83: 721-32.

1604 Seymour RS, White CR. 2011. Can the basal metabolic rate of endotherms be explained by
1605 biophysical modeling? Response to "a new model for the body size-metabolism relationship".
1606 *Physiological and biochemical zoology* 84: 107-10.

1607 Smith, R.E. 1956. Quantitative relations between liver mitochondria metabolism and total body
1608 weight in mammals. *Annals of the New York Academy of Sciences* 62: 403-421.

1609 Sousa T, Domingos T, Poggiale JC, Kooijman SA. 2010. Dynamic energy budget theory restores
1610 coherence in biology. *Philosophical transactions of the Royal Society of London. Series B,*
1611 *Biological sciences* 365: 3413-28.

1612 Taylor GK, Nudds RL, Thomas AL. 2003. Flying and swimming animals cruise at a Strouhal
1613 number tuned for high power efficiency. *Nature* 425: 707-11.

1614 Walker EP. 1968. *Mammals of the World*. Baltimore. John Hopkins.

1615 Wang Z, O'Connor TP, Heshka S, Heymsfield SB. 2001. The reconstruction of Kleiber's law at
1616 the organ-tissue level. *The Journal of nutrition* 131: 2967-70.

1617 West GB, Brown JH, Enquist BJ. 1997. A general model for the origin of allometric scaling laws
1618 in biology. *Science* 276: 122-126.

1619 White CR, Seymour RS. 2003. Mammalian basal metabolic rate is proportional to body mass2/3.
1620 *Proceedings of the National Academy of Sciences of the United States of* America 100: 4046-9.

1621 White CR, Blackburn TM, Seymour RS. 2009. Phylogenetically informed analysis of the
1622 allometry of Mammalian Basal metabolic rate supports neither geometric nor quarter-power
1623 scaling. *Evolution; international journal of organic evolution* 63: 2658-67.

1624 White, C.R. There is no single p. 2010. Nature 464: 691.

1625 White CR, Kearney MR, Matthews PG, Kooijman SA, Marshall DJ. 2011. A manipulative test
1626 of competing theories for metabolic scaling. *The American naturalist* 178: 746-54.

1627 White CR, Frappell PB, Chown SL. 2012. An information-theoretic approach to evaluating the
1628 size and temperature dependence of metabolic rate. *Proceedings. Biological sciences / The*
1629 *Royal Society* 279: 3616-21

1630 White CR, Kearney MR. 2013. Determinants of inter-specific variation in basal metabolic rate.
1631 *Journal of comparative physiology. B, Biochemical, systemic, and environmental physiology*
1632 183: 1-26